
Protecting Sensitive Data through Federated Co-Training

Amr Abourayya^{1,2} Jens Kleesiek¹ Kanishka Rao³ Erman Ayday⁴ Bharat Rao³ Geoffrey I. Webb⁵
Michael Kamp^{1,2,5}

Abstract

In many applications, sensitive data is inherently distributed and may not be pooled due to privacy concerns. Federated learning allows us to collaboratively train a model without pooling the data by iteratively aggregating the parameters of local models. It is possible, though, to infer upon the sensitive data from the shared model parameters. We propose to use a federated co-training approach where clients share hard labels on a public unlabeled dataset instead of model parameters. A consensus on the shared labels forms a pseudo labeling for the unlabeled dataset that clients use in combination with their private data to train local models. We show that sharing hard labels substantially improves privacy over sharing model parameters. At the same time, federated co-training achieves a model quality comparable to federated learning. Moreover, it allows us to use local models such as (gradient boosted) decision trees, rule ensembles, and random forests that do not lend themselves to the parameter aggregation used in federated learning.

1. Introduction

Can we substantially improve privacy in collaborative machine learning from distributed sensitive datasets? Federated learning (FEDAVG) (McMahan et al., 2017) allows distributed sites to collaboratively train a joint model without directly disclosing their sensitive data by instead periodically sharing and aggregating parameters of locally trained models. However, it is possible for an attacker or curious ob-

server to make non-trivial inferences about local data from model parameters (Ma et al., 2020) and model updates (Zhu & Han, 2020). This poses a severe threat to sensitive data.

We propose to use a federated form of co-training (Zhou & Li, 2005; Rasmus et al., 2015) where clients iteratively share predictions on an unlabeled public dataset. A server forms a consensus of these predictions, and clients use this consensus as pseudo-labels for the unlabeled dataset in their local training. A straightforward consensus mechanism for classification problems is a majority vote. In this federated co-training (FEDCT), clients share only *hard labels* (Galstyan & Cohen, 2007), e.g., via one-hot encoded classifications, and thereby improve privacy substantially over sharing model parameters in classical federated learning: Fig. 1 shows that FEDCT reduces the empirical vulnerability to membership inference attacks substantially over FEDAVG while maintaining similar model quality. Sharing hard labels has not only privacy benefits, but also allows us to use arbitrary supervised learning methods at each client, including interpretable models, such as decision trees (Quinlan, 1986) or XGBoost (Friedman, 2001; Chen & Guestrin, 2016). We analyze the convergence of FEDCT and provide a novel result showing that hard label sharing converges with high probability under the condition that local training accuracies increase between communication rounds.

Instead of sharing hard labels, it has previously been proposed to share *soft labels* (Galstyan & Cohen, 2007), e.g., the probability vector over classes. In distributed distillation (DD) (Bistriz et al., 2020) these soft labels are used for a co-regularization term (Sindhwani et al., 2005; Ullrich et al., 2017) that promotes agreement between clients. Sharing only soft labels also improves privacy over FEDAVG, but less than sharing hard labels (Fig. 1).

Instead of sharing less information we can also add a tailored noise to the shared information to improve privacy. This allows us to give strong theoretical guarantees in terms of differential privacy (Wei et al., 2020) (DP), e.g., via Gaussian (Geyer et al., 2017) or Laplacian (Dwork et al., 2006) noise on model parameters in FEDAVG (Wei et al., 2020). This differentially private federated averaging (DP-FEDAVG), however, reduces model quality, resulting in a trade-off between privacy and quality that is typically

¹Institute for AI in medicine (IKIM), University Hospital Essen, Germany ²Institute for Neuroinformatics, Ruhr University Bochum, Germany ³Carenostics, Pennsylvania, USA ⁴Case Western Reserve University, Cleveland, USA ⁵Department of Data Science & AI, Monash University, Melbourne, Australia. Correspondence to: Amr Abourayya <amr.abourayya@uk-essen.de>, Michael Kamp <michael.kamp@uk-essen.de>.

poor: Xiao et al. (2022) show that using an amount of noise in differentially private distributed SGD such that the resulting model still has decent quality has slim to no actual privacy (i.e., $\epsilon = 145, \delta = 10^{-5}$) (Xiao et al., 2022)¹. Our experiments confirm this: DP-FEDAVG improves privacy slightly (Fig. 1) at the cost of model quality (on average a drop of more than 13% in test accuracy, whereas FEDCT has virtually the same accuracy).

Hard label sharing empirically improves privacy, but it makes achieving differential privacy guarantees—the current gold standard in privacy (Ziller et al., 2021; Chaudhuri et al., 2019)—challenging: for classification, the shared information is discrete and therefore standard noise mechanisms (e.g. Gaussian, Laplacian) cannot be applied. Instead, we apply an XOR-mechanism (Ji et al., 2021) on one-hot-encoded predictions. To obtain a DP guarantee, this requires a bound on the sensitivity, i.e., the change in predictions on the unlabeled dataset if a single element in the training set is altered. We provide a novel bound on this sensitivity for all local learning algorithms that are on-average-leave-one-out-stable. The resulting differentially private FEDCT (DP-FEDCT) retains high model quality while providing strong DP guarantees. We empirically observe that the locally applied perturbations on average do not impact the consensus substantially—similar robustness of majority votes has been observed for noise on the class counts (Papernot et al., 2017). Thus, FEDCT achieves high model quality with strong DP guarantees.

We empirically compare FEDCT against FEDAVG, DP-FEDAVG, and DD in terms of global test accuracy and vulnerability to membership inference attacks on three benchmark datasets (CIFAR10, FashionMNIST, SVHN) and two real-world medical datasets (Pneumonia, MRI), showing that FEDCT protects privacy almost optimally while achieving a model quality similar to FEDAVG and DD, and outperforming DP-FEDAVG.

In summary, our contributions are

- (i) a novel federated co-training (FEDCT) approach to collaboratively train models from privacy-sensitive distributed data sources via hard label sharing on a public unlabeled dataset that achieves model quality comparable to standard federated learning and distributed distillation and can seamlessly integrate any supervised learning method on clients in the federated system, including interpretable models, such as XGboost, decision trees, Random forest, and rule ensembles;
- (ii) a theoretical analysis providing a novel convergence result for hard label sharing, and a novel sensitivity

¹The probability of an adversary learning about an individual from a dataset of size n is $\gtrsim n^{-1}e^\epsilon$ (Lee & Clifton, 2011)

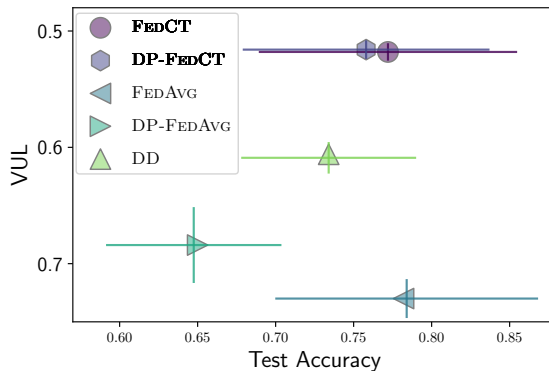


Figure 1: Vulnerability (VUL) to membership inference attacks on the communication of 5 clients and their test accuracy (avg and std over 5 datasets). VUL is measured empirically as the success probability of inferring membership correctly, $VUL = 0.5$ implies optimal privacy.

bound for hard label sharing by on-average-leave-one-out-stable machine learning algorithms to provide DP guarantees for FEDCT using the XOR-mechanism;

- (iii) an extensive empirical evaluation showing that FEDCT achieves a favorable privacy-utility trade-off compared to model parameter and soft label sharing.

2. Related Work

We discuss related work on privacy in federated learning as well as distributed semi-supervised learning that fit our scenario. We discuss more distantly related work in App. C.

Privacy in Federated Learning: Collaboratively training a model without sharing sensitive data is a key advantage of (horizontal) federated learning (McMahan et al., 2017) which trains local models and aggregates their parameters periodically. Communicating only model parameters for aggregation, however, does not entirely protect local data: An attacker or curious observer can make inferences about local data from model parameters (Shokri et al., 2017; Ma et al., 2020) and model updates (Zhu & Han, 2020). Should a malicious client obtain model updates through additional attacks, a common defense is perturbing shared information, e.g., applying appropriate clipping and noise before sending models. This can guarantee ϵ, δ -differential privacy for local data (Wei et al., 2020) at the cost of model quality. This technique is also proven to defend against backdoor and poisoning attacks (Sun et al., 2019). Truex et al. (2019) proposes enhancing the privacy of data exchange in traditional distributed algorithms through the use of secure multi-party communication (SMPC) and differential privacy (DP). While this enables the application of both classical

distributed decision tree algorithms and federated learning methods, SMPC has scalability and efficiency limitations and DP involves a trade-off between privacy and utility. In scenarios where SMPC is applicable (and the same holds for homomorphic encryption (Roth et al., 2019) and trusted execution environments (Subramanian et al., 2017)), it offers an additional level of privacy that can be combined with the above federated and semi-supervised approaches (cf. Sec. 4 in Kairouz et al., 2021).

Distributed semi-supervised learning: Semi-supervised learning utilizes both labeled and unlabeled data (Zhou & Li, 2005; Rasmus et al., 2015) for training. In centralized co-training classifiers are independently trained on distinct feature sets, or views, of labeled data and their consensus on unlabeled data is used as pseudo-labels (Blum & Mitchell, 1998; Ullrich et al., 2017). Papernot et al. (2017) propose a distributed—but not collaborative—knowledge distillation approach called PATE where teachers are trained distributedly and a consensus of their predictions on the unlabeled data is used to train a student model. We empirically compare to PATE and its differentially private variant DP-PATE in App. D.3. Bistriz et al. (2020) propose to share soft predictions on unlabeled data to reduce communication in federated (and decentralized) deep learning and term their approach distributed distillation (DD). We compare to DD, showing that we achieve similar model quality and communication with improved privacy. Chen & Chao (2020) employ knowledge distillation to train a student model based on predictions from a Bayesian model ensemble (FedBE). Similarly, (Lin et al., 2020)’s FedDF also uses knowledge distillation in a federated context to create a global model by fusing client models. Both FedBE and FedDF require sharing local model parameters and thus have the same privacy issues that FEDAVG has.

3. Federated Semi-Supervised Learning

3.1. Preliminaries

We assume learning algorithms $\mathcal{A} : \mathcal{X} \times \mathcal{Y} \rightarrow \mathcal{H}$ that produce models $h \in \mathcal{H}$ using a dataset $D \subset \mathcal{X} \times \mathcal{Y}$ from an input space \mathcal{X} and output space \mathcal{Y} , i.e., $h_{t+1} = \mathcal{A}(D)$, or iterative learning algorithms (cf. Chp. 2.1.4 Kamp, 2019) $\mathcal{A} : \mathcal{X} \times \mathcal{Y} \times \mathcal{H} \rightarrow \mathcal{H}$ that update a model $h_{t+1} = \mathcal{A}(D, h_t)$. Given a set of $m \in \mathbb{N}$ clients with local datasets $D^1, \dots, D^m \subset \mathcal{X} \times \mathcal{Y}$ drawn iid from a data distribution \mathcal{D} and a loss function $\ell : \mathcal{Y} \times \mathcal{Y} \rightarrow \mathbb{R}$, the goal is to find a set of local models $h^{1*}, \dots, h^{m*} \in \mathcal{H}$ that each minimize the risk

$$\varepsilon(h) = \mathbb{E}_{(x,y) \sim \mathcal{D}}[\ell(h(x), y)] . \quad (1)$$

In *centralized learning*, datasets are pooled as $D = \bigcup_{i \in [m]} D^i$ and \mathcal{A} is applied to D until convergence. Note that applying \mathcal{A} on D can be the application to any random

subset, e.g., as in mini-batch training, and convergence is measured in terms of low training loss, small gradient, or small deviation from previous iterations. In standard *federated learning* (McMahan et al., 2017), \mathcal{A} is applied in parallel for $b \in \mathbb{N}$ rounds on each client locally to produce local models h^1, \dots, h^m . These models are then centralized and aggregated using an aggregation operator $\text{agg} : \mathcal{H}^m \rightarrow \mathcal{H}$, i.e., $\bar{h} = \text{agg}(h^1, \dots, h^m)$. The aggregated model \bar{h} is then redistributed to local clients which perform another b rounds of training using \bar{h} as a starting point. This is iterated until convergence of \bar{h} . When aggregating by averaging, this method is known as federated averaging (FEDAVG).

In federated semi-supervised learning, a public unlabeled dataset U is available to all clients. Clients can share predictions on U (both hard and soft labels), as well as model parameters. Since sharing model parameters threatens privacy, we consider semi-supervised approaches that share predictions (other approaches are discussed in App. C).

3.2. A Federated Co-Training Approach

Algorithm 1: Federated Co-Training (FEDCT)

Input: communication period b , m clients with local datasets D^1, \dots, D^m and local learning algorithms $\mathcal{A}^1, \dots, \mathcal{A}^m$, unlabeled shared dataset U , total number of rounds T

Output: final models h_T^1, \dots, h_T^m

```

1 initialize local models  $h_0^1, \dots, h_0^m$ ,  $P \leftarrow \emptyset$ 
2 Locally at client  $i$  at time  $t$  do
3    $h_t^i \leftarrow \mathcal{A}^i(D^i \cup P, h_{t-1}^i)$ 
4   if  $t \% b = b - 1$  then
5      $L_t^i \leftarrow h_t^i(U)$ 
6     send  $L_t^i$  to server and receive  $L_t$ 
7      $P \leftarrow (U, L_t)$ 
8   end
9 At server at time  $t$  do
10  receive local pseudo-labels  $L_t^1, \dots, L_t^m$ 
11   $L_t \leftarrow \text{consensus}(L_t^1, \dots, L_t^m)$ 
12  send  $L_t$  to all clients
    
```

We propose a federated form of co-training (Blum & Mitchell, 1998) that iteratively updates a pseudo-labeling of U via the consensus of shared predictions. That is, in a communication round $t \in \mathbb{N}$ each client $i \in [m]$ shares local labels $L_t^i = h_t^i(U)$ (not soft predictions) on U with the server, which produces a consensus labeling $L_t \subset \mathcal{Y}$ via an appropriate consensus mechanism. The resulting pseudo-labeled dataset $P = (U, L_t)$ augments local training sets. We call this approach federated co-training (FEDCT). Sharing hard labels not only improves privacy, but also allows us to use any supervised learning method for local training.

We describe federated co-training in Algorithm 1: at each

client i , the local model is updated using local dataset D^i combined with the current pseudo-labeled public dataset P (line 4). In a communication round (line 5), the updated model is used to produce improved pseudo-labels L^i for the unlabeled data U (line 6), which are sent to a server (line 7). At the server, when all local prediction L^1, \dots, L^m are received (line 12), a consensus L is formed (line 13) and broadcasted to the clients (14). At the client, upon receiving the consensus labels (line 8), the pseudo-labeled dataset is updated (line 9), and another iteration of local training is performed. For classification problems the majority vote is a reliable consensus mechanism (Papernot et al., 2017).

Convergence Analysis: The convergence of federated co-training depends on the convergence of the local learning algorithms $(\mathcal{A}^i)_{i \in [m]}$. Under the assumption that these algorithms converge on a fixed training set, it remains to show that there is a time from which the training set does not change anymore. That is, there exists a round $t_0 \in \mathbb{N}$ such that for all $t > t_0$ it holds that $L_t = L_{t-1}$. For classification problems, this depends on the local training accuracy. If local training accuracy reaches $a_t = 1.0$, then the approach trivially converges, since local models will reproduce L_t in every subsequent round. This assumption can usually be fulfilled for over-parameterized models. In the following, we show that the approach also converges with high probability, if the training accuracy is ≤ 1 , but linearly increasing with t .

Proposition 1. *For $m \geq 3$ clients with local datasets D^1, \dots, D^m and unlabeled dataset U , let \mathcal{A}^i for $i \in [m]$ be a set of learning algorithms that all achieve a linearly increasing training accuracy a_t for all labelings of U , i.e., there exists $c \in \mathbb{R}_+$ such that $a_t \geq 1 - c/t$, then there exists $t_0 \in \mathbb{N}$ such that $a_t \geq 1/2$ and FEDCT with majority vote converges with probability $1 - \delta$, where*

$$\delta \leq |U| (4c)^{\frac{m}{2}} \zeta\left(\frac{m}{2}, t_0 + 1\right)$$

and $\zeta(x, q)$ is the Hurwitz zeta function.

Proof. (sketch:) We show that if local models are of sufficient quality, then in round $t \geq t_0$, the probability that the consensus labels change, δ_t , is bounded. Indeed, the probability can be determined via the CDF of the binomial distribution, which can be bounded via the Chernoff bound, yielding

$$\delta_t \leq |U| 4^{\frac{m}{2}} a_t^{\frac{m}{2}} (1 - a_t)^{\frac{m}{2}}.$$

We then show that the probability that the consensus labels remain constant for the remainder, i.e., the sum of δ_t from t_0 to ∞ , is bounded as well. Using the assumption that a_t grows linearly, we can express this infinite series as

$$\sum_{t=t_0}^{\infty} \delta_t \lesssim \sum_{t=0}^{\infty} \frac{1}{t^{\frac{m}{2}}} - \sum_{t=0}^{t_0} \frac{1}{t^{\frac{m}{2}}},$$

that is, the difference of the Riemann zeta function and the t_0 -th generalized harmonic number, $\sum_{t=t_0}^{\infty} \delta_t \lesssim \zeta(m/2) - H_{t_0}^{m/2}$. This difference can be expressed via the Hurwitz zeta function $\zeta(m/2, t_0 + 1)$. \square

The full proof is provided in Appendix A. Note that $\delta \rightarrow 0$ for $t_0 \rightarrow \infty$, and δ is monotonically decreasing with m . To illustrate this result, we plotted δ wrt. t_0 in Figure 2. It shows that for moderate numbers of clients ($m \geq 50$) we obtain convergence with probability ≈ 1.0 at $t_0 = 1000$ (for $m = 50$ and $m = 100$ with $c \in \{1, 2, 10\}$). For cross-silo scenarios ($m = 5$) it depends on how fast the local accuracy increases: $\delta = 0.9962$ for $c = 1$, but $\delta = 0.7868$ for $c = 10$.

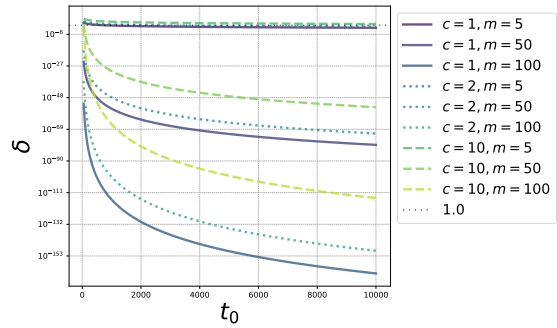


Figure 2: Numerical evaluation of the upper bound on δ in Prop. 1 for $|U| = 10^4$.

Communication Complexity: The communication complexity of FEDCT is in the same order as standard federated learning, i.e., treating the message size as a constant, the communication complexity is in $\mathcal{O}(T/b)$, where b is the communication period. The actual number of bits transferred in each round, however, depends on the size of U : Encoding predictions as binary vectors, for a classification problem with $C \in \mathbb{N}$ classes the communication complexity is in $\mathcal{O}(TC|U|/b)$. As Bistriz et al. (2020) observed, transferring predictions on U can reduce communication substantially over transferring the weights of large neural networks. For example on FashionMINST with $|U| = 10^4$ and a neural network with 669 706 parameters (cf. Tab. 1), FEDCT and FEDAVG both achieve a test accuracy of 0.82, resp. 0.83, but FEDCT transmits only $\approx 12.2KB$ bits in each round, whereas FEDAVG transmits $\approx 2.6MB$. Thus, FEDCT reduces communication by a factor of ≈ 214 .

4. Differential Privacy for FEDCT

For our privacy analysis, we assume the following attack model: clients are honest and the server may be honest-but-curious (or semi-honest, i.e., it follows the protocol

execution correctly, but may try to infer sensitive information about the clients). The main goal of an attacker is to infer sensitive information about the local training data of the clients from shared information. This assumption is stronger than an attacker intercepting individual communication, or an honest-but-curious client, since the server receives the most information from clients during the protocol. We also assume that parties do not collude. Details are referred to Appendix E.1. Sharing hard labels on an unlabeled dataset empirically improves the privacy of sensitive local data substantially², as we show in Section 5. An empirical improvement in privacy is, however, no guarantee. Differential privacy instead provides a fundamental guarantee of privacy which is achieved through randomization of shared information.

Definition 1 ((Dwork et al., 2014)). *A randomized mechanism \mathcal{M} with domain \mathcal{X} and range \mathcal{Y} is ϵ -differential private if for any two neighboring inputs $D, D' \subset \mathcal{X}$ and for a subset of outputs $S \in \mathcal{Y}$ it holds that*

$$P(\mathcal{M}(D) \in S) \leq \exp(\epsilon)P(\mathcal{M}(D') \in S) .$$

To obtain differential privacy (DP), the randomization has to be suitable to the information that is shared. In FEDCT local clients share hard labels, i.e., categorical values in case of classification. Standard DP mechanisms, like the Gaussian (Dwork et al., 2014) or Laplacian mechanism (Dwork et al., 2006) are not suitable for categorical data. Therefore, we interpret labels as binary vectors via one-hot encoding. We then use a DP mechanism for binary data that is based on computing the XOR operation of the original data and a random binary matrix (Ji et al., 2021).

The XOR-Mechanism (Ji et al., 2021): For an unlabeled dataset U and a classification problem with $C \in \mathbb{N}$ classes, the predictions sent by a client with local dataset $D \subset \mathcal{X}$ to the server can be interpreted as the binary matrix output of a deterministic mechanism $f(D) \in \{0, 1\}^{|U| \times C}$. Given two neighboring datasets D, D' (i.e., they differ only in a single element), the sensitivity of f is defined as $s_f = \sup_{f(D), f(D')} \|f(D) \oplus f(D')\|_F^2$, where \oplus denotes binary XOR. Now let $\mathcal{B} \in \{0, 1\}^{N \times P}$ to denote a matrix-valued Bernoulli random variable, i.e., $\mathcal{B} \sim \text{Ber}_{N,P}(\Theta, \Lambda_{1,2}, \dots, \Lambda_{N-1,N})$ with a matrix-valued Bernoulli distribution with quadratic exponential dependence structure. Here, Θ is the $P \times P$ association parametric matrix including log-linear parameters describing the association structure of the columns, and $\Lambda_{i,j}$ is the $P \times P$ association parametric matrix of rows i and j . The XOR-mechanism applies this random matrix to the output of the deterministic mechanism via the XOR operator \oplus and

²Note that this differs from label leakage (Li & Zhang, 2021), where predictions on the private data are shared.

yields a randomized mechanism $\mathcal{M}(D) = f(D) \oplus \mathcal{B}$. Applying this XOR-mechanism to federated co-training means representing local predictions L_t^i as binary matrices and producing randomized predictions $\widehat{L}_t^i = L_t^i \oplus \mathcal{B}$ that are then sent to the server, resulting in differentially private distributed co-training (DP-FEDCT): Defining the sensitivity of DP-FEDCT as $s_* = \max\{s_{f^1}, \dots, s_{f^m}\}$, it follows directly from Theorem 1 in Ji et al. (2021) that DP-FEDCT achieves ϵ -differential privacy.

Corollary 1. *Applying XOR mechanism to FEDCT with sensitivity s_* achieves ϵ -DP if Θ and $\Lambda_{i,j}$ satisfy*

$$s_*(\|\lambda(\Theta)\|_2 + \sum_{i=1}^{N-1} \sum_{j=i+1}^N \|\lambda(\Lambda_{i,j})\|_2) \leq \epsilon, \quad (2)$$

where $\|\lambda(\Theta)\|_2$ and $\|\lambda(\Lambda_{i,j})\|_2$ are the l_2 norms of the eigenvalues of Θ and $\Lambda_{i,j}$.

To compute an actual guarantee, we need to bound the sensitivity of FEDCT, i.e., bound how much the predictions of a client on the unlabeled dataset can change if one element of its local training set is removed. In the following, we bound the sensitivity of any learning algorithm that is on-average-replace-one-stable.

Definition 2 ((Shalev-Shwartz & Ben-David, 2014)). *(On-Average-Replace-One-Stable) Let $\epsilon : \mathbb{N} \rightarrow \mathbb{R}$ be a monotonically decreasing function, and ℓ a loss function. We say that a learning algorithm \mathcal{A} is on-average-replace-one-stable with rate $\epsilon(m)$ if for every distribution \mathcal{D}*

$$\mathbb{E}_{\substack{(S, z') \sim \mathcal{D}^{m+1} \\ i \sim U(m)}} \left[\ell(\mathcal{A}(S^{(i)}, z_i)) - \ell(\mathcal{A}(S), z_i) \right] \leq \epsilon(m).$$

Using this definition, we obtain the following bound for the sensitivity.

Proposition 2. *For classification models $h : \mathcal{X} \rightarrow \mathcal{Y}$, let ℓ be a loss function that upper bounds the 0-1-loss and \mathcal{A} a learning algorithm that is on-average-replace-one stable with stability rate $\epsilon(m)$ for ℓ . Let $D \cup U$ be a local training set with $|U| = n$, and $\delta \in (0, 1)$. Then with probability $1 - \delta$, the sensitivity s_* of \mathcal{A} on U is bounded by*

$$s_* \leq \left[n\epsilon(n) + P\sqrt{n\epsilon(n)(1 - \epsilon(n))} + \frac{P^2}{3} \right],$$

where $P = \Phi^{-1}(1 - \delta)$ and Φ^{-1} is the probit function.

The proof is provided in Appendix B. On-average-replace-one-stability holds for many supervised learning methods. For example, every regularized risk minimizer for a convex, Lipschitz loss using a strongly convex regularizer, like Thikonov-regularization, is on-average-replace-one-stable (cf. Chp. 13.3 in Shalev-Shwartz & Ben-David, 2014). We empirically evaluate the privacy-utility trade-off of FEDCT with differential privacy in Sec. 5.

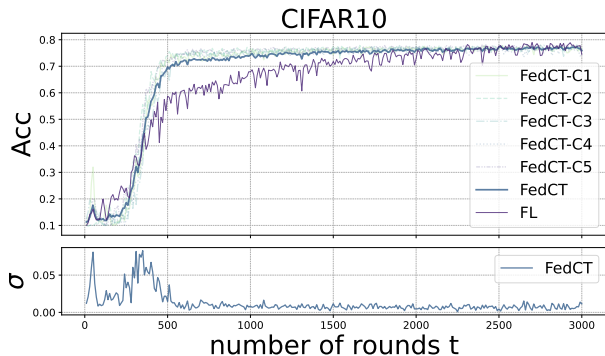


Figure 3: **Top:** Test accuracy (ACC) over time on CIFAR10 with ACC of FL, and ACC of local models and their average for FEDCT. **Bottom:** Standard deviation of test accuracy of local models in FEDCT.

5. Empirical Evaluation

We empirically show that federated co-training presents a more favorable privacy-utility trade-off compared to federated learning by showing that it achieves similar test accuracy with substantially improved privacy. We compare FEDCT to standard federated averaging (McMahan et al., 2017) (FEDAVG), differentially private federated averaging (DP-FEDAVG) achieved via the Gaussian mechanism to FEDAVG (Geyer et al., 2017), and distributed distillation (Bistriz et al., 2020) (DD)³ on 3 benchmark datasets and 2 medical image classification datasets, as well as on a fine-tuning task for large language models.

Experimental Setup We use the three benchmark image classification datasets, CIFAR10 (Krizhevsky et al., 2010), FashionMNIST (Xiao et al., 2017), and SVHN (Netzer et al., 2011), as well as two real medical image classification datasets, MRI scans for brain tumor detection (Chakrabarty, 2018), and chest X-rays for pneumonia detection (Kermary et al., 2018). We evaluate FEDCT with interpretable models on five benchmark datasets, WineQuality (Cortez et al., 2009), Breastcancer (Street et al., 1993), AdultsIncome (Becker & Kohavi, 1996), Mushroom (Bache & Lichman, 1987), and Covertypes (Blackard, 1998). We fine-tune an LLM on the IMDB dataset (Maas et al., 2011). We first divide each dataset into a test and training set and further divide the training set into an unlabeled dataset U and a set of m local training sets (sampling iid. for all experiments, except for the experiments on heterogeneous data distributions). The architectures of the neural networks are provided in Appendix E. The hyper-parameters are optimized individually for all methods on a subset of the training set via cross-validation. We select the number of rounds to be the

³The code is available at <https://anonymous.4open.science/r/federatedcotraining-B03C>

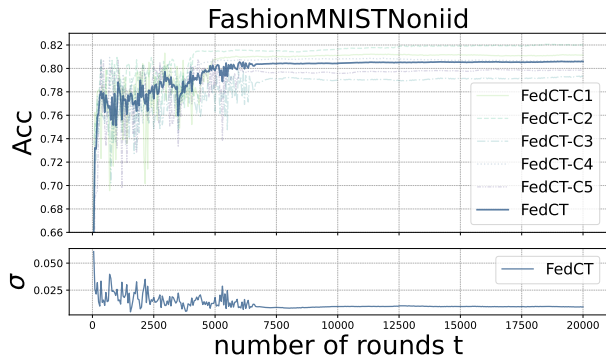


Figure 4: **Top:** Test accuracy (ACC) over time for $m = 5$ local models of FEDCT on heterogeneous distribution for the FashionMNIST dataset ($\alpha_1 = 100, \alpha_2 = 2$). **Bottom:** Standard deviation of test accuracy of local models in FEDCT.

maximum rounds required so that all methods converge, i.e., $T = 2 \cdot 10^4$. We measure empirical privacy vulnerability by performing a large number of membership inference attacks and compute the probability of inferring upon sensitive data, using the ML Privacy Meter tool (Murakonda & Shokri, 2020). The **vulnerability (VUL)** of a method is the ROC AUC of membership attacks over K runs over the entire training set. A vulnerability of 1.0 means that membership can be inferred with certainty, whereas 0.5 means that deciding on membership is a random guess.

Privacy-Utility-Trade-Off: We first evaluate the performance of FEDCT and baselines for deep learning on homogeneous data distributions. We use an unlabeled dataset of size $|U| = 10^4$ for CIFAR10, $|U| = 5 \cdot 10^4$ for FashionMNIST, $|U| = 170$ for MRI, $|U| = 900$ for Pneumonia, and $|U| = 35 \cdot 10^4$ for SVHM. Note that only FEDCT, DP-FEDCT, and DD use the unlabeled dataset. The remaining training data is distributed over $m = 5$ clients. We repeat all experiments 3 times and report average test accuracy and standard deviation. Further details are deferred to App. E.

The results presented in Table 1 show that FEDCT achieves a test accuracy comparable to both FEDAVG and DD, while preserving privacy to the highest level. That is, FEDCT performs best on CIFAR10, has a similar performance to both on FashionMNIST, Pneumonia, and SVHN, and is slightly worse on MRI. The vulnerability is around 0.5, so that membership inference attacks are akin to random guessing. FEDAVG instead consistently has a vulnerability over 0.7. DP-FEDAVG improves privacy, but also reduces the test accuracy substantially. Our experiments show that DD substantially improves privacy over both FEDAVG and DP-FEDAVG, yet it is still vulnerable ($VUL \approx 0.6$). Since FEDCT does not produce a global model, we investigate the convergence behavior of individual client models in

Dataset	FEDCT		DP-FEDCT ($\epsilon = 0.1$)		FEDAVG		DP-FEDAVG ($\epsilon = 0.1$)		DD	
	ACC	VUL	ACC	VUL	ACC	VUL	ACC	VUL	ACC	VUL
CIFAR10	0.77 \pm 0.003	0.52	0.76 \pm 0.002	0.51	0.77 \pm 0.020	0.73	0.68 \pm 0.002	0.70	0.67 \pm 0.012	0.61
FashionMNIST	0.82 \pm 0.004	0.51	0.80 \pm 0.001	0.52	0.83 \pm 0.024	0.72	0.69 \pm 0.002	0.71	0.82 \pm 0.016	0.60
Pneumonia	0.76 \pm 0.008	0.51	0.75 \pm 0.004	0.51	0.74 \pm 0.013	0.76	0.61 \pm 0.004	0.69	0.77 \pm 0.003	0.63
MRI	0.63 \pm 0.004	0.52	0.62 \pm 0.002	0.51	0.66 \pm 0.015	0.73	0.56 \pm 0.003	0.62	0.68 \pm 0.008	0.60
SVHN	0.88 \pm 0.002	0.53	0.86 \pm 0.001	0.53	0.91 \pm 0.026	0.71	0.71 \pm 0.005	0.70	0.73 \pm 0.014	0.59

 Table 1: Test accuracy (ACC) and privacy vulnerability (VUL, smaller is better) for $m = 5$ clients on iid data.

terms of test accuracy on CIFAR10 in Figure 3. From the standard deviation between clients σ we see that they converge to a consensus after around 700 rounds with only slight deviations afterward. Overall, FEDCT converges slightly faster than FEDAVG, though the latter increases its test accuracy slightly further, eventually.

Privacy-Utility Trade-Off With Differential Privacy:

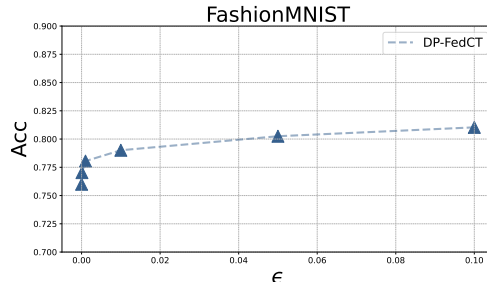
Differential privacy guarantees typically come at a cost in terms of utility, which in our case means a loss in model quality. Analyzing this privacy-utility trade-off requires estimating the sensitivity. Since stability-bounds for neural networks tend to underestimate the on-average-replace-one stability, leading to vacuous results for generalization (Nagarajan & Kolter, 2019; Petzka et al., 2021), using them to bound sensitivity would underestimate utility. Using an empirical approximation provides a more accurate estimate for the privacy-utility trade-off (Rubinstein & Aldà, 2017). To get this approximation, we apply FEDCT with $m = 5$ clients on the FashionMNIST dataset (Xiao et al., 2017) for various privacy levels ϵ . We estimate the sensitivity of DP-FEDCT by sampling $n = 100$ datasets D'_1, \dots, D'_n neighboring a local training set D to approximate

$$s_* \approx \max_{i \in [n]} \|f(D) \oplus f(D'_i)\|_F^2,$$

which yields $s_* \approx 3000$. Using this estimate, Figure 5 shows that DP-FEDCT achieves a high utility in terms of test accuracy even for moderate-to-high privacy levels ϵ with an accuracy of 0.8 for $\epsilon = 0.1$ ⁴ (without any noise, FEDCT achieves an accuracy of 0.82 in this setup). As Papernot et al. (2017) observed, the reason for the good trade-off probably lies in the consensus mechanism: for a single unlabeled example $\mu > m/C$ clients predict the majority class, so the XOR-mechanism has to change the predictions of at least $\mu - m/C$ many clients to change its consensus label.

Heterogeneous Data Distributions: In most realistic applications, local datasets are not iid distributed. While this is not the main focus of this work, we show that FEDCT performs similar to FEDAVG for non-pathological non-iid

⁴Note that using the trivial upper bound of $s_*^W = |U| = 5 \cdot 10^4$ instead of our estimate results in a slightly higher epsilon: for a noise level that achieves $\epsilon = 0.1$ with the empirical estimate of s_* , the worst-case bound results in $\epsilon = 0.1 \cdot s_*^W / s_* = 5/3$, instead.


 Figure 5: Accuracy (ACC) of DP-FEDCT on the FashionMNIST dataset under different levels of privacy ϵ .

Dirichlet α_1, α_2	FEDCT	FEDAVG	DD
$\alpha_1 = 100, \alpha_2 = 2$	0.81	0.82	0.80
$\alpha_1 = 100, \alpha_2 = 0.01$	0.80	0.79	0.79
$\alpha_1 = \alpha_2 = 0.01$	0.37	0.73	0.36

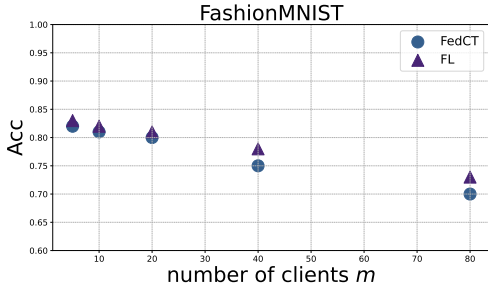
Table 2: Average test accuracy on non-iid data distributions.

data distributions, but label sharing (both hard and soft) performs poorly on pathological non-iid distributions. For a non-pathological non-iid data distribution, we sample half of the training data from a Dirichlet distribution over labels with $\alpha_1 = 100$ (mild heterogeneity) and the other half with $\alpha_2 = 2$ (medium heterogeneity) and $\alpha_2 = 0.01$ (strong heterogeneity). For both cases, we see that FEDCT, DD, and FEDAVG perform similarly. In Fig. 4 we show the convergence behavior of individual clients for $\alpha_1 = 100, \alpha_2 = 2$ which is similar to the iid case, but with higher variance between individual client models. For the pathological case ($\alpha_1 = \alpha_2 = 0.01$) FEDAVG still performs well, but both FEDCT and DD perform poorly. We conjecture that a meaningful consensus can only be formed if clients achieve a minimum performance for all labels. In the pathological case, clients observe only a small subset of labels and thus perform poorly on a majority of data.

Scalability: We test the scalability of FEDCT in terms of the number of clients on FashionMNIST, using the same setup as before. We increase the number of clients $m \in \{5, 10, 20, 40, 80\}$ and keep the overall training set size constant, so for larger numbers of clients the local training set size decreases. The results in Figure 6 show that higher levels of distribution reduce the accuracy slightly, but

Dataset	DT		RuleFit		XGBoost		Random Forest	
	FEDCT	CENTRALIZED	FEDCT	CENTRALIZED	FEDCT	CENTRALIZED	FEDCT	CENTRALIZED
WineQuality	0.95 ± 0.010	0.92	0.93 ± 0.012	0.95	0.94 ± 0.010	0.94	0.96 ± 0.011	0.98
BreastCancer	0.89 ± 0.012	0.89	0.92 ± 0.011	0.93	0.93 ± 0.010	0.94	0.90 ± 0.021	0.93
AdultsIncome	0.81 ± 0.014	0.82	0.84 ± 0.020	0.85	0.85 ± 0.021	0.87	0.85 ± 0.010	0.86
Mushroom	0.98 ± 0.013	1.00	0.98 ± 0.022	1.00	0.98 ± 0.012	1.00	0.99 ± 0.013	1
Coverttype	0.88 ± 0.020	0.94	0.73 ± 0.021	0.76	0.84 ± 0.022	0.87	0.90 ± 0.013	0.95

Table 3: Test accuracy of interpretable models trained via FEDCT and centralized training.

Figure 6: Test accuracy (ACC) of FEDCT and FEDAVG FashionMNIST with $|U| = 5 \cdot 10^5$ for various m .

both FEDCT and FEDAVG show only a moderate decline, with FEDAVG performing slightly better than FEDCT.

Interpretable Models: A major benefit of FEDCT is that it allows training models that cannot be aggregated in FEDAVG and cannot be trained via soft label sharing (e.g., as in DD). Many interpretable models, such as decision trees (Quinlan, 1986), XGBoost (Chen & Guestrin, 2016), Random Forest (Breiman, 2001), and RuleFit (Friedman & Popescu, 2008) fall under this class. We evaluate FEDCT with these models on 5 benchmark datasets with $m = 5$ clients and compare its performance to pooling all data and training a model centrally (Centralized). The results in Table 3 show that FEDCT can train interpretable models in a federated learning setup, achieving a model quality comparable to centralized training. In App. D.1 we show that FEDCT can also train mixed models, i.e., each client training a different model type, to high accuracy.

Fine-Tuning Large Language Models: In fine-tuning, model quality is already high at the beginning of training, which suits co-training well—the pseudo-labels produced are likely to be of high quality from the start. If true, semi-supervised approaches benefit from the unlabeled dataset and should improve performance over FEDAVG. To test this hypothesis, we fine-tune the GPT2 model transformer with a sequence classification head (linear layer) comprising 124.44 million parameters on the IMBD sentimental dataset (Maas et al., 2011) using $m = 10$ clients with $|U| = 150$. Indeed, we observe that FEDCT achieves a test accuracy of 0.73, whereas FEDAVG achieves an ACC

of 0.59. Details can be found in App. D.2.

6. Discussion and Conclusion

We propose a semi-supervised, federated co-training approach that collaboratively trains models via sharing predictions on an unlabeled dataset U . While such an unlabeled dataset is not always available, in many applications, such as healthcare, they are available⁵ or can be synthetically generated (El Emam et al., 2020).

A limitation of FEDCT is that it does not produce a global model. Instead, it promotes agreement between local models. While our experiments show that local models quickly converge to similar test accuracy, we cannot guarantee their similarity. At the same time, FEDCT allows us to use different models that can be tailored to each client (see App. D.1). A second limitation, revealed by our experiments, is that hard and soft label sharing performs poorly on pathological non-iid data, where clients only observe a small subset of labels. Here, FEDAVG achieves a decent performance. Moreover, FL methods tailored to heterogeneous data, such as FedProx (Li et al., 2020) or SCAFFOLD (Karimireddy et al., 2020), typically perform even better. Investigating whether more elaborate consensus mechanisms (Warfield et al., 2004) improve FEDCT’s performance in that case makes for excellent future work. Furthermore, investigating client subsampling in FEDCT and its impact on the consensus mechanism, other communication-efficient strategies (e.g., Kamp et al., 2016; 2019), and learning from small datasets (Kamp et al., 2023) is interesting. The results on fine-tuning LLMs are promising and suggest that semi-supervised learning can be beneficial in federated fine-tuning of foundation models. These preliminary experiments are, however, not conclusive, yet. It will be interesting to investigate FEDCT for fine-tuning in the future.

We show both theoretically and empirically that FEDCT achieves a model quality comparable to FEDAVG and DD, while improving privacy over both FEDAVG and DD, as well as DP-FEDAVG. From this we conclude that sharing hard labels improves privacy substantially while maintaining

⁵In healthcare, large public health databases are quite common: US NCHS databases, UK NHS databases, UK Biobank (Sudlow et al., 2015), MIMIC-III database (Johnson et al., 2016), TCGA public dataset (NIH, 2011), and the planned European EHDS.

a favorable privacy-utility trade-off. Moreover, FEDCT allows us to train interpretable models, such as decision trees, rule of ensembles, XGBoost, and random forest in a federated learning setup.

7. Impact Statements

This paper tackles the problem of privacy in collaborative and federated learning. While federated learning allows us to collaboratively train models without sharing sensitive data directly, attackers can still make non-trivial inference about sensitive data from the shared information, such as model parameters, model updates, or gradients.

This is not only a hypothetical issue. The example of healthcare shows the necessity of collaborative training, but also the importance of ensuring privacy: Despite isolated successes for ML in healthcare for early detection to improve outcomes and reduce costs (Keen et al., 2018; Fenton et al., 2013; Rao et al., 2007), widespread adoption of ML to support clinical decisions remains distant. A critical barrier is access to large and diverse patient data. Modern ML techniques, if given access to millions of records collected in routine care from multiple institutions, are capable of learning robust, high-performing models for disease that identify novel markers of risk, predict disease to help clinicians intervene earlier, model disease progression and even suggest preventative interventions for individual patients (Chittora et al., 2021; Khan et al., 2020; Qin et al., 2020; Sree & Ramesh, 2020). Unfortunately, privacy (HIPAA) and other regulatory and reputational concerns prevent medical institutions from sharing patient data to create large representative patient datasets for training (The Office for Civil Rights (OCR) and Bradley Malin, 2012; Blackmer, 2016; Seh et al., 2020; Editor, 2019). Federated learning improves privacy over data pooling. Its privacy vulnerability is considered a major challenge in healthcare, though (Rieke et al., 2020), that prevents its widespread application. Our research can help resolving the privacy issues in collaborative training and thereby unlock machine learning on large, distributed, yet highly sensitive datasets, as in healthcare.

To illustrate the potential impact of training high-quality ML models collaboratively in healthcare, consider chronic disease. The US healthcare costs are projected to grow from an estimated \$3.8 trillion in 2020 to \$6.2 trillion by 2028 - with a significant portion of this growth driven by chronic disease. Six in ten Americans live with at least one chronic disease, and seven of the top 10 causes of death were related to chronic disease. Chronic conditions and costs are particularly severe in the elderly populations, with 8 in 10 Americans over 65 suffering from multiple chronic conditions (Lochner & Cox, 2013; Nowakowski et al., 2019), and are commonly undertreated in minority populations.

Advances in clinical care, formulary therapeutics, and behavior modification can slow disease progression, prevent complications, curb rising costs and prevent needless suffering, *provided diagnosis of chronic disease occurs in early stages* (more than a third of costs and suffering associated with the \$1 trillion are avoidable) (Waters & Marlon, 2018). Unfortunately, most chronic diseases remain undiagnosed until late stages (e.g., 50% of CVD (60M) patients and 40% of COPD (12M) patients are undiagnosed),(CDC, 2020; CMS.gov, 2019) when therapy costs are significantly higher and therapy impact on disease progression is greatly diminished. Machine learning methods have the potential to detect chronic disease early and automatically. That has the potential to radically transform healthcare into a tech-driven paradigm where insights learned from millions of patient records are used to identify novel markers of risk, predict disease to help clinicians intervene earlier, model disease progression, and eventually, make precision medicine a reality by tailoring treatment and preventative interventions to individual patients.

References

- Bache, K. and Lichman, M. Mushroom. UCI Machine Learning Repository, 1987. DOI: <https://doi.org/10.24432/C5959T>.
- Becker, B. and Kohavi, R. Adult. UCI Machine Learning Repository, 1996. DOI: <https://doi.org/10.24432/C5XW20>.
- Bistriz, I., Mann, A., and Bambos, N. Distributed distillation for on-device learning. *Advances in Neural Information Processing Systems*, 33:22593–22604, 2020.
- Blackard, J. Covertypes. UCI Machine Learning Repository, 1998. DOI: <https://doi.org/10.24432/C50K5N>.
- Blackmer, W. S. Eu general data protection regulation (gdpr). *Official Journal of the European Union*, 2014, 2016.
- Blum, A. and Mitchell, T. Combining labeled and unlabeled data with co-training. In *Proceedings of the eleventh annual conference on computational learning theory*, pp. 92–100, 1998.
- Breiman, L. Random forests. *Machine learning*, 45:5–32, 2001.
- CDC. Health and economic costs of chronic disease. *National Center for Chronic Disease Prevention and Health Promotion*, 2020.
- Chakrabarty, N. Brain tumor detection, kaggle, 2018. URL <https://www.kaggle.com/datasets/navoneel/brain-mri-images-for-brain-tumor-detection>.
- Chaudhuri, K., Imola, J., and Machanavajjhala, A. Capacity bounded differential privacy. *Advances in Neural Information Processing Systems*, 32, 2019.
- Chen, H., Vikalo, H., et al. The best of both worlds: Accurate global and personalized models through federated learning with data-free hyper-knowledge distillation. *International Conference on Learning Representations ICLR*, 2023.
- Chen, H.-Y. and Chao, W.-L. Fedbe: Making bayesian model ensemble applicable to federated learning. In *International Conference on Learning Representations*, 2020.
- Chen, T. and Guestrin, C. Xgboost: A scalable tree boosting system. In *Proceedings of the 22nd acm sigkdd international conference on knowledge discovery and data mining*, pp. 785–794, 2016.
- Chittora, P., Chaurasia, S., Chakrabarti, P., Kumawat, G., Chakrabarti, T., Leonowicz, Z., Jasinski, M., Jasinski, L., Gono, R., Jasinska, E., and Bolshev, V. Prediction of chronic kidney disease -a machine learning perspective. *IEEE Access*, 2021.
- Cho, Y. J., Manoel, A., Joshi, G., Sim, R., and Dimitriadis, D. Heterogeneous ensemble knowledge transfer for training large models in federated learning. *Proceedings of the Thirty-First International Joint Conference on Artificial Intelligence (IJCAI)*, 2022.
- Cho, Y. J., Wang, J., Chirvolu, T., and Joshi, G. Communication-efficient and model-heterogeneous personalized federated learning via clustered knowledge transfer. *IEEE Journal of Selected Topics in Signal Processing*, 17(1):234–247, 2023.
- CMS.gov. National health expenditures 2019 highlights. *Center for Medicaid and Medicare Services*, 2019.
- Cortez, P., Cerdeira, A., Almeida, F., Matos, T., and Reis, J. Modeling wine preferences by data mining from physicochemical properties. *Decision support systems*, 47(4): 547–553, 2009.
- Dekel, O., Gilad-Bachrach, R., Shamir, O., and Xiao, L. Optimal distributed online prediction using mini-batches. *Journal of Machine Learning Research*, 13(1), 2012.
- Diao, E., Ding, J., and Tarokh, V. Semifl: Semi-supervised federated learning for unlabeled clients with alternate training. *Advances in Neural Information Processing Systems*, 35:17871–17884, 2022.
- Dwork, C., McSherry, F., Nissim, K., and Smith, A. Calibrating noise to sensitivity in private data analysis. In *Theory of Cryptography: Third Theory of Cryptography Conference, TCC 2006, New York, NY, USA, March 4-7, 2006. Proceedings 3*, pp. 265–284. Springer, 2006.
- Dwork, C., Roth, A., et al. The algorithmic foundations of differential privacy. *Foundations and Trends® in Theoretical Computer Science*, 9(3–4):211–407, 2014.
- Editor, H. J. Healthcare data breach statistics. *HIPAA Journal*, 2019.
- El Emam, K., Mosquera, L., and Hoptroff, R. *Practical synthetic data generation: balancing privacy and the broad availability of data*. O’Reilly Media, 2020.
- Fenton, J. J., Xing, G., Elmore, J. G., Bang, H., Chen, S. L., Lindfors, K. K., and Baldwin, L. M. Short-term outcomes of screening mammography using computer-aided detection a population-based study of medicare enrollees. *Annals of Internal Medicine*, 158, 2013.
- Friedman, J. H. Greedy function approximation: a gradient boosting machine. *Annals of statistics*, pp. 1189–1232, 2001.

- Friedman, J. H. and Popescu, B. E. Predictive learning via rule ensembles. *The annals of applied statistics*, pp. 916–954, 2008.
- Galstyan, A. and Cohen, P. R. Empirical comparison of “hard” and “soft” label propagation for relational classification. In *International Conference on Inductive Logic Programming*, pp. 98–111. Springer, 2007.
- Geyer, R. C., Klein, T., and Nabi, M. Differentially private federated learning: A client level perspective. *arXiv preprint arXiv:1712.07557*, 2017.
- Itahara, S., Nishio, T., Koda, Y., Morikura, M., and Yamamoto, K. Distillation-based semi-supervised federated learning for communication-efficient collaborative training with non-iid private data. *IEEE Transactions on Mobile Computing*, 22(1):191–205, 2021.
- Ji, T., Li, P., Yilmaz, E., Ayday, E., Ye, Y., and Sun, J. Differentially private binary-and matrix-valued data query: an xor mechanism. *Proceedings of the VLDB Endowment*, 14(5):849–862, 2021.
- Johnson, A., Pollard, T., and Mark, R. Mimic-iii clinical database (version 1.4). *PhysioNet*, 10:C2XW26, 2016.
- Kairouz, P., McMahan, H. B., Avent, B., Bellet, A., Bennis, M., Bhagoji, A. N., Bonawitz, K., Charles, Z., Cormode, G., Cummings, R., et al. Advances and open problems in federated learning. *Foundations and Trends® in Machine Learning*, 14(1–2):1–210, 2021.
- Kamp, M. *Black-Box Parallelization for Machine Learning*. PhD thesis, Rheinische Friedrich-Wilhelms-Universität Bonn, Universitäts- und Landesbibliothek Bonn, 2019.
- Kamp, M., Boley, M., Keren, D., Schuster, A., and Sharfman, I. Communication-efficient distributed online prediction by dynamic model synchronization. In *Machine Learning and Knowledge Discovery in Databases: European Conference, ECML PKDD 2014, Nancy, France, September 15-19, 2014. Proceedings, Part I 14*, pp. 623–639. Springer, 2014.
- Kamp, M., Bothe, S., Boley, M., and Mock, M. Communication-efficient distributed online learning with kernels. In *Machine Learning and Knowledge Discovery in Databases: European Conference, ECML PKDD 2016, Riva del Garda, Italy, September 19-23, 2016. Proceedings, Part II 16*, pp. 805–819. Springer, 2016.
- Kamp, M., Adilova, L., Sicking, J., Hüger, F., Schlicht, P., Wirtz, T., and Wrobel, S. Efficient decentralized deep learning by dynamic model averaging. In *Machine Learning and Knowledge Discovery in Databases: European Conference, ECML PKDD 2018, Dublin, Ireland, September 10–14, 2018. Proceedings, Part I 18*, pp. 393–409. Springer, 2019.
- Kamp, M., Fischer, J., and Vreeken, J. Federated learning from small datasets. In *The Eleventh International Conference on Learning Representations*, 2023.
- Karimireddy, S. P., Kale, S., Mohri, M., Reddi, S., Stich, S., and Suresh, A. T. Scaffold: Stochastic controlled averaging for federated learning. In *International Conference on Machine Learning*, pp. 5132–5143. PMLR, 2020.
- Keen, J. D., Keen, J. M., and Keen, J. E. Utilization of computer-aided detection for digital screening mammography in the united states, 2008 to 2016. *Journal of the American College of Radiology*, 15, 2018.
- Kermany, D. S., Goldbaum, M., Cai, W., Valentim, C. C., Liang, H., Baxter, S. L., McKeown, A., Yang, G., Wu, X., Yan, F., et al. Identifying medical diagnoses and treatable diseases by image-based deep learning. *cell*, 172(5):1122–1131, 2018.
- Khan, B., Naseem, R., Muhammad, F., Abbas, G., and Kim, S. An empirical evaluation of machine learning techniques for chronic kidney disease prophecy. *IEEE Access*, 8, 2020.
- Krizhevsky, A., Nair, V., and Hinton, G. Cifar-10 (canadian institute for advanced research), 2010.
- Lee, J. and Clifton, C. How much is enough? choosing ϵ for differential privacy. In *Information Security*, pp. 325–340. Springer, 2011.
- Li, D. and Wang, J. Fedmd: Heterogenous federated learning via model distillation. *arXiv preprint arXiv:1910.03581*, 2019.
- Li, Q., He, B., and Song, D. Model-contrastive federated learning. In *Proceedings of the IEEE/CVF conference on computer vision and pattern recognition*, pp. 10713–10722, 2021.
- Li, T., Sahu, A. K., Zaheer, M., Sanjabi, M., Talwalkar, A., and Smith, V. Federated optimization in heterogeneous networks. In *Proceedings of Machine learning and systems*, volume 2, pp. 429–450, 2020.
- Li, Z. and Zhang, Y. Membership leakage in label-only exposures. In *Proceedings of the 2021 ACM SIGSAC Conference on Computer and Communications Security*, pp. 880–895, 2021.
- Lin, H., Lou, J., Xiong, L., and Shahabi, C. Semifed: Semi-supervised federated learning with consistency and pseudo-labeling. *arXiv preprint arXiv:2108.09412*, 2021.
- Lin, T., Kong, L., Stich, S. U., and Jaggi, M. Ensemble distillation for robust model fusion in federated learning. *Advances in Neural Information Processing Systems*, 33: 2351–2363, 2020.

- Lochner, K. A. and Cox, C. S. Prevalence of multiple chronic conditions among medicare beneficiaries, united states, 2010. *Preventing Chronic Disease*, 10, 2013.
- Ma, C., Li, J., Ding, M., Yang, H. H., Shu, F., Quek, T. Q., and Poor, H. V. On safeguarding privacy and security in the framework of federated learning. *IEEE network*, 34 (4):242–248, 2020.
- Maas, A. L., Daly, R. E., Pham, P. T., Huang, D., Ng, A. Y., and Potts, C. Learning word vectors for sentiment analysis. In *Proceedings of the 49th Annual Meeting of the Association for Computational Linguistics: Human Language Technologies*, pp. 142–150, Portland, Oregon, USA, June 2011. Association for Computational Linguistics.
- McDonald, R., Mohri, M., Silberman, N., Walker, D., and Mann, G. Efficient large-scale distributed training of conditional maximum entropy models. *Advances in neural information processing systems*, 22, 2009.
- McMahan, B., Moore, E., Ramage, D., Hampson, S., and y Arcas, B. A. Communication-efficient learning of deep networks from decentralized data. In *Artificial intelligence and statistics*, pp. 1273–1282. PMLR, 2017.
- Murakonda, S. K. and Shokri, R. Ml privacy meter: Aiding regulatory compliance by quantifying the privacy risks of machine learning. *arXiv preprint arXiv:2007.09339*, 2020.
- Nagarajan, V. and Kolter, J. Z. Uniform convergence may be unable to explain generalization in deep learning. *Advances in Neural Information Processing Systems*, 32, 2019.
- Netzer, Y., Wang, T., Coates, A., Bissacco, A., Wu, B., and Ng, A. Y. Reading digits in natural images with unsupervised feature learning, 2011.
- NIH, N. C. I. The cancer genome atlas program (tcga), 2011. URL <https://www.cancer.gov/tcga>.
- Nowakowski, A. C., Shin, J., and Carretta, H. J. Regional risk: Mapping single and multiple chronic conditions in the united states. *SAGE Open*, 9, 2019.
- Papernot, N., Abadi, M., Erlingsson, U., Goodfellow, I., and Talwar, K. Semi-supervised knowledge transfer for deep learning from private training data. *International Conference on Learning Representations ICLR*, 2017.
- Petzka, H., Kamp, M., Adilova, L., Sminchisescu, C., and Boley, M. Relative flatness and generalization. *Advances in neural information processing systems*, 34: 18420–18432, 2021.
- Qin, J., Chen, L., Liu, Y., Liu, C., Feng, C., and Chen, B. A machine learning methodology for diagnosing chronic kidney disease. *IEEE Access*, 8, 2020.
- Quinlan, J. R. Induction of decision trees. *Machine learning*, 1:81–106, 1986.
- Rao, R. B., Bi, J., Fung, G., Salganicoff, M., Obuchowski, N., and Naidich, D. Lungcad: A clinically approved, machine learning system for lung cancer detection. In *Proceedings of the ACM SIGKDD International Conference on Knowledge Discovery and Data Mining*, 2007.
- Rasmus, A., Berglund, M., Honkala, M., Valpola, H., and Raiko, T. Semi-supervised learning with ladder networks. *Advances in neural information processing systems*, 28, 2015.
- Rieke, N., Hancox, J., Li, W., Milletari, F., Roth, H. R., Albarqouni, S., Bakas, S., Galtier, M. N., Landman, B. A., Maier-Hein, K., et al. The future of digital health with federated learning. *NPJ digital medicine*, 3(1):119, 2020.
- Roth, E., Noble, D., Falk, B. H., and Haeberlen, A. Honeycrisp: large-scale differentially private aggregation without a trusted core. In *Proceedings of the 27th ACM Symposium on Operating Systems Principles*, pp. 196–210, 2019.
- Rubinstein, B. I. and Aldà, F. Pain-free random differential privacy with sensitivity sampling. In *International Conference on Machine Learning*, pp. 2950–2959. PMLR, 2017.
- Seh, A. H., Zarour, M., Alenezi, M., Sarkar, A. K., Agrawal, A., Kumar, R., and Khan, R. A. Healthcare data breaches: Insights and implications. *Healthcare (Switzerland)*, 8, 2020. ISSN 22279032. doi: 10.3390/healthcare8020133.
- Shalev-Shwartz, S. and Ben-David, S. *Understanding machine learning: From theory to algorithms*. Cambridge university press, 2014.
- Shokri, R., Stronati, M., Song, C., and Shmatikov, V. Membership inference attacks against machine learning models. In *2017 IEEE symposium on security and privacy (SP)*, pp. 3–18. IEEE, 2017.
- Short, M. On binomial quantile and proportion bounds: With applications in engineering and informatics. *Communications in Statistics-Theory and Methods*, 52(12): 4183–4199, 2023.
- Sindhwani, V., Niyogi, P., and Belkin, M. A co-regularization approach to semi-supervised learning with multiple views. In *Proceedings of ICML workshop on learning with multiple views*, volume 2005, pp. 74–79. Citeseer, 2005.

- Sree, S. R. and Ramesh, S. N. Artificial intelligence aided diagnosis of chronic kidney disease. *Journal of Critical Reviews*, 7, 2020.
- Street, W. N., Wolberg, W. H., and Mangasarian, O. L. Nuclear feature extraction for breast tumor diagnosis. In *Biomedical image processing and biomedical visualization*, volume 1905, pp. 861–870. SPIE, 1993.
- Subramanyan, P., Sinha, R., Lebedev, I., Devadas, S., and Seshia, S. A. A formal foundation for secure remote execution of enclaves. In *Proceedings of the 2017 ACM SIGSAC conference on computer and communications security*, pp. 2435–2450, 2017.
- Sudlow, C., Gallacher, J., Allen, N., Beral, V., Burton, P., Danesh, J., Downey, P., Elliott, P., Green, J., Landray, M., et al. Uk biobank: an open access resource for identifying the causes of a wide range of complex diseases of middle and old age. *PLoS medicine*, 12(3):e1001779, 2015.
- Sun, Z., Kairouz, P., Suresh, A. T., and McMahan, H. B. Can you really backdoor federated learning? *arXiv preprint arXiv:1911.07963*, 2019.
- The Office for Civil Rights (OCR) and Bradley Malin. Guidance regarding methods for de-identification of protected health information in accordance with the health insurance portability and accountability act (hipaa) privacy rule. *Health Information Privacy*, 2012.
- Truex, S., Baracaldo, N., Anwar, A., Steinke, T., Ludwig, H., Zhang, R., and Zhou, Y. A hybrid approach to privacy-preserving federated learning. In *Proceedings of the 12th ACM workshop on artificial intelligence and security*, pp. 1–11, 2019.
- Ullrich, K., Kamp, M., Gärtner, T., Vogt, M., and Wrobel, S. Co-regularised support vector regression. In *Machine Learning and Knowledge Discovery in Databases: European Conference, ECML PKDD 2017, Skopje, Macedonia, September 18–22, 2017, Proceedings, Part II 10*, pp. 338–354. Springer, 2017.
- Warfield, S. K., Zou, K. H., and Wells, W. M. Simultaneous truth and performance level estimation (staple): an algorithm for the validation of image segmentation. *IEEE transactions on medical imaging*, 23(7):903–921, 2004.
- Waters, H. and Marlon, G. The costs of chronic disease in the u.s. *Milken Institute*, 2018.
- Wei, K., Li, J., Ding, M., Ma, C., Yang, H. H., Farokhi, F., Jin, S., Quek, T. Q., and Poor, H. V. Federated learning with differential privacy: Algorithms and performance analysis. *IEEE Transactions on Information Forensics and Security*, 15:3454–3469, 2020.
- Xiao, H., Rasul, K., and Vollgraf, R. Fashion-mnist: a novel image dataset for benchmarking machine learning algorithms, 2017.
- Xiao, H., Wan, J., and Devadas, S. Differentially private deep learning with modelmix. *arXiv preprint arXiv:2210.03843*, 2022.
- Zhou, Z.-H. and Li, M. Tri-training: Exploiting unlabeled data using three classifiers. *IEEE Transactions on Knowledge and Data Engineering*, 17(11):1529–1541, 2005.
- Zhu, L. and Han, S. Deep leakage from gradients. In *Federated learning*, pp. 17–31. Springer, 2020.
- Zhu, Z., Hong, J., and Zhou, J. Data-free knowledge distillation for heterogeneous federated learning. In *International conference on machine learning*, pp. 12878–12889. PMLR, 2021.
- Ziller, A., Usynin, D., Braren, R., Makowski, M., Rueckert, D., and Kaissis, G. Medical imaging deep learning with differential privacy. *Scientific Reports*, 11(1):13524, 2021.

A. Proof of Proposition 1

For convenience, we restate the proposition.

Proposition 1. For $m \geq 3$ clients with local datasets D^1, \dots, D^m and unlabeled dataset U , let \mathcal{A}^i for $i \in [m]$ be a set of learning algorithms that all achieve a linearly increasing training accuracy a_t for all labelings of U , i.e., there exists $c \in \mathbb{R}_+$ such that $a_t \geq 1 - c/t$, then there exists $t_0 \in \mathbb{N}$ such that $a_t \geq 1/2$ and FEDCT with majority vote converges with probability $1 - \delta$, where

$$\delta \leq |U|(4c)^{\frac{m}{2}} \zeta\left(\frac{m}{2}, t_0 + 1\right)$$

and $\zeta(x, q)$ is the Hurwitz zeta function.

Proof. Let P_t denote the consensus label at time $t \in \mathbb{N}$. We first show that the probability δ_t of $P_t \neq P_{t-1}$ is bounded. Since the learning algorithm \mathcal{A} at time $t \geq t_0$ achieves a training accuracy $a_t \geq 0.5$, the probability can be determined via the CDF of the binomial distribution, i.e.,

$$\begin{aligned} \delta_t &= \mathbb{P}\left(\exists u \in U : \sum_{i=1}^m \mathbb{1}_{h_t^i(u)=v} < \left\lfloor \frac{m}{2} \right\rfloor\right) \\ &= F\left(\left\lfloor \frac{m}{2} \right\rfloor - 1, m, a_t\right) = \sum_{i=1}^{\lfloor \frac{m}{2} \rfloor - 1} \binom{m}{i} a_t^i (1 - a_t)^{m-i}. \end{aligned}$$

Where v is the consensus label at $t - 1$. Note that this is a worst-case bound, since for $C > 2$ a majority can be achieved already with $\lfloor m/C \rfloor$ many votes. If any class gets at least $m/2$ votes, though, for any number of classes it is guaranteed that it is the majority. Applying the Chernoff bound and denoting by $D(\cdot \parallel \cdot)$ the Kullback-Leibler divergence yields

$$\begin{aligned} \delta_t &\leq \exp\left(-mD\left(\frac{\lfloor \frac{m}{2} \rfloor - 1}{m} \parallel a_t\right)\right) \\ &= \exp\left(-m\left(\frac{\lfloor \frac{m}{2} \rfloor - 1}{m} \log \frac{\lfloor \frac{m}{2} \rfloor - 1}{a_t} + \left(1 - \frac{\lfloor \frac{m}{2} \rfloor - 1}{m}\right) \log \frac{1 - \frac{\lfloor \frac{m}{2} \rfloor - 1}{m}}{1 - a_t}\right)\right) \\ &\leq \exp\left(-m\left(\frac{\frac{m}{2}}{m} \log \frac{\frac{m}{2}}{a_t} + \left(1 - \frac{\frac{m}{2}}{m}\right) \log \frac{1 - \frac{\frac{m}{2}}{m}}{1 - a_t}\right)\right) \\ &= \exp\left(-m\left(\frac{1}{2} \log \frac{1}{2a_t} + \frac{1}{2} \log \frac{1}{2(1 - a_t)}\right)\right) = \exp\left(-\frac{m}{2} \log \frac{1}{2a_t} - \frac{m}{2} \log \frac{1}{2(1 - a_t)}\right) \\ &= \exp\left(\frac{m}{2} (\log 2a_t + \log 2(1 - a_t))\right) = (2a_t)^{\frac{m}{2}} (2(1 - a_t))^{\frac{m}{2}} = 4^{\frac{m}{2}} a_t^{\frac{m}{2}} (1 - a_t)^{\frac{m}{2}}. \end{aligned}$$

The union bound over all $u \in U$ yields

$$\delta_t \leq |U| 4^{\frac{m}{2}} a_t^{\frac{m}{2}} (1 - a_t)^{\frac{m}{2}}.$$

To show convergence, we need to show that for $t_0 \in \mathbb{N}$ it holds that

$$\sum_{t=t_0}^{\infty} \delta_t \leq \delta$$

for $0 \leq \delta < 1$. Since we assume that a_t grows linearly, we can write wlog. $a_t = 1 - c/t$ for some $c \in \mathbb{R}_+$ and $t \geq 2c$. With this, the sum can be written as

$$\begin{aligned} \sum_{t=t_0}^{\infty} \delta_t &\leq |U| \sum_{t=t_0}^{\infty} 4^{\frac{m}{2}} \left(1 - \frac{c}{t}\right)^{\frac{m}{2}} \left(\frac{c}{t}\right)^{\frac{m}{2}} = |U| 4^{\frac{m}{2}} \sum_{t=t_0}^{\infty} \left(\frac{t-1}{\frac{t^2}{c^2}}\right)^{\frac{m}{2}} \\ &\leq |U| 4^{\frac{m}{2}} \sum_{t=t_0}^{\infty} \left(\frac{t}{\frac{t^2}{c^2}}\right)^{\frac{m}{2}} = (4c)^{\frac{m}{2}} \sum_{t=t_0}^{\infty} \left(\frac{1}{t}\right)^{\frac{m}{2}} = |U| (4c)^{\frac{m}{2}} \zeta\left(\frac{m}{2}\right) - H_{t_0}^{\left(\frac{m}{2}\right)}, \end{aligned}$$

where $\zeta(x)$ is the Riemann zeta function and $H_n^{(x)}$ is the generalized harmonic number. Note that $H_n^{(x)} = \zeta(x) - \zeta(x, n+1)$, where $\zeta(x, q)$ is the Hurwitz zeta function, so that this expression can be simplified to

$$\sum_{t=t_0}^{\infty} \delta_t \leq |U|(4c)^{\frac{m}{2}} \zeta\left(\frac{m}{2}\right) - \zeta\left(\frac{m}{2}\right) + \zeta\left(\frac{m}{2}, t_0 + 1\right) = |U|(4c)^{\frac{m}{2}} \zeta\left(\frac{m}{2}, t_0 + 1\right) .$$

□

B. Proof of Proposition 2

For convenience, we restate the proposition.

Proposition 2. *For classification models $h : \mathcal{X} \rightarrow \mathcal{Y}$, let ℓ be a loss function that upper bounds the 0 – 1-loss and \mathcal{A} a learning algorithm that is on-average-replace-one stable with stability rate $\epsilon(m)$ for ℓ . Let $D \cup U$ be a local training set with $|U| = n$, and $\delta \in (0, 1)$. Then with probability $1 - \delta$, the sensitivity s_* of \mathcal{A} on U is bounded by*

$$s_* \leq \left[n\epsilon(n) + P\sqrt{n\epsilon(n)(1 - \epsilon(n))} + \frac{P^2}{3} \right] ,$$

where $P = \Phi^{-1}(1 - \delta)$ and Φ^{-1} is the probit function.

Proof. The sensitivity s_* is defined as the supremum of the Frobenius norm of the symmetric difference between the predictions on the unlabeled dataset U for two models h_s and $h_{s'}$ trained on datasets s and s' that differ by one instance.

$$s_* = \sup_{S, S'} \|h_S(U) \Delta h_{S'}(U)\|_F$$

Since \mathcal{A} is on-average-replace-one stable with rate ϵ for ℓ and ℓ upper bounds the 0 – 1-loss, \mathcal{A} is on-average-replace-one stable with rate at most ϵ for the 0 – 1-loss. Thus, the expected change in loss on a single element of the training set is bounded by $\epsilon(|D \cup U|)$. Since the 0 – 1-loss is either 0 or 1, this can be interpreted as a success probability in a Bernoulli process. The expected number of differences on the unlabeled dataset then is the expected value of the corresponding binomial distribution, i.e., $|U|\epsilon(|D \cup U|) \leq |U|\epsilon(|U|)$. We are interested in the maximum number of successes such that the cumulative distribution function of the binomial distribution is smaller than $1 - \delta$. This threshold k can be found using the quantile function (inverse CDF) for which, however, no closed form exists. [Short \(2023\)](#) has shown that the quantile function $Q(n, p, R)$ can be bounded by

$$Q(n, p, R) \leq \left[np + \Phi^{-1}(R)\sqrt{np(1-p)} + \frac{\Phi^{-1}(R)^2}{3} \right] ,$$

where Φ^{-1} is the probit function (inverse of standard normal's cdf). With $n = |u|$, $p = \epsilon(|U|)$, and $R = 1 - \delta$, the number of differences in predictions on the unlabeled dataset, i.e., the sensitivity s_* , is upper bounded by

$$s_* \leq \left[|U|\epsilon(|U|) + \Phi^{-1}(1 - \delta)\sqrt{|U|\epsilon(|U|)(1 - \epsilon(|U|))} + \frac{\Phi^{-1}(1 - \delta)^2}{3} \right]$$

with probability $1 - \delta$.

□

C. Additional Related Work

The main goal of FEDCT is to improve the privacy of current federated learning approaches while maintaining model quality. For that, we consider a classical FL scenario where clients hold a private local dataset. We additionally assume that they have access to a public unlabeled dataset.

In federated learning, clients share the parameters of local models (or model update / gradients) with a server that aggregates them. Averaging model parameters and gradients has been proposed first for maximum-entropy models [McDonald et al. \(2009\)](#) and has been investigated in online learning [Dekel et al. \(2012\)](#); [Kamp et al. \(2014\)](#). [McMahan et al. \(2017\)](#)

Protecting Sensitive Data through Federated Co-Training

Method	Shared Information	Allow Heterogeneity	Public Data	Train Non-Gradient Methods	Collaborative Training
FedAvg (McMahan et al., 2017)	model Parameters	no	none	no	yes
FedHKD (Chen et al., 2023)	model parameters, representations, soft labels	no	none	no	yes
FedMD (Li & Wang, 2019)	soft labels	yes	labeled	no	yes
SemiFL (Diao et al., 2022)	model parameters	no	unlabeled	no	yes
SemiFed (Lin et al., 2021)	model parameters	no	unlabeled	no	yes
FedDF (Lin et al., 2020)	model parameters, soft labels	yes	unlabeled	no	yes
DD (Bistriz et al., 2020)	soft labels	yes	unlabeled	no	yes
PATE (Papernot et al., 2017)	hard labels	yes	unlabeled	yes	no
FedCT (ours)	hard labels	yes	unlabeled	yes	yes

Table 4: Comparison of Different Federated Learning Methods

proposed averaging gradients and model parameters in deep learning (FEDAVG). A variety of methods have improved the performance of FEDAVG by altering the local objective function or the aggregation, in particular for heterogeneous data. For example, FedProx (Li et al., 2020) adds a regularizer to the local loss function that promotes proximity to the last model aggregate, SCAFFOLD (Karimireddy et al., 2020) adds control variables to the local optimization that account for client drift, MOON (Li et al., 2021) which uses a form of self-supervised learning to improve local models via a contrastive loss function, or FedGen (Zhu et al., 2021) which learns a data generator from the shared model parameters that generates additional training data for clients. While these methods improve performance, in particular on heterogeneous data, they require sharing model parameters (and sometimes additional information) and therefore have at least the same privacy drawbacks that FEDAVG has.

Semi-supervised federated learning uses an unlabeled public dataset to share (additional) information. We discussed semi-supervised approaches that fit our scenario, i.e., that only share predictions on an unlabeled dataset, in Sec. 2. There are, however, semi-supervised federated learning methods that do not directly fit our scenario or do not improve over the baselines we selected. For example, Fed-ET (Cho et al., 2022), semiFed (Lin et al., 2021), SemiFL (Diao et al., 2022), FedGen (Zhu et al., 2021), and FedHKD (Chen et al., 2023) (also) share model parameters and therefore do not improve privacy over FEDAVG. Cho et al. (2023) propose to use co-regularization for personalized federated learning. For non-personalized FL this approach is equivalent to distributed distillation (DD) (Bistriz et al., 2020). The approach proposed by Itahara et al. (2021) is also similar to DD. FedMD (Li & Wang, 2019) uses a public labeled dataset and therefore does not fit our scenario. Since the heterogeneous data setup they proposed is interesting, though, we nonetheless compare it to FEDCT in App. D.4. Similarly, PATE Papernot et al. (2017) is not collaborative and therefore also does not directly fit our scenario, as discussed in Sec. 2. Moreover, its privacy mechanism does not protect against an honest-but-curious server. However, since the approach is similar to FEDCT in that it shares hard labels on an unlabeled dataset, we do compare PATE and its differentially private variant DP-PATE to FEDCT in App. D.3.

In Tab. 4 we provide an overview over the methods mentioned that highlights what information is shared by the method, whether it allows for model heterogeneity (i.e., whether clients may use different models), if and what type of public dataset is used, whether the method can train non-gradient-based models, such as decision trees, and whether the method is collaborative (i.e., whether clients learn from each other, or a single model is distilled from clients, instead).

D. Additional Empirical Evaluation

In this section, we provide further details on our experiments, as well as additional results that further investigate the properties of FEDCT. First, we demonstrate FEDCT’s ability to collaboratively train clients that each use different models, e.g., one using a decision tree, another a neural network, etc. We then provide additional details on our experiment on fine-tuning a large language model with FEDCT. We also compare FEDCT with two more distantly related baselines, PATE and FedMD: PATE also shares hard labels like FEDCT, but is not collaborative, and FedMD shares soft labels and requires a labeled public dataset (see Tab. 4 in Sec. C). To investigate the effect of co-training, we perform an ablation study in which we investigate the impact of the size of the unlabeled dataset on FEDCT’s performance and compare FEDCT’s performance to local training. Lastly, we provide an additional result on the scalability of FEDCT in terms of the number of clients.

D.1. Mixed Model Types

Sharing hard labels allows us to train any supervised learning method on each client. This means, we can even use different model types for different clients in FEDCT. To demonstrate this, we compare using the best performing interpretable model on every client—for the BreatCancer dataset that is XGBoost—to two heterogeneous ensembles using different combinations

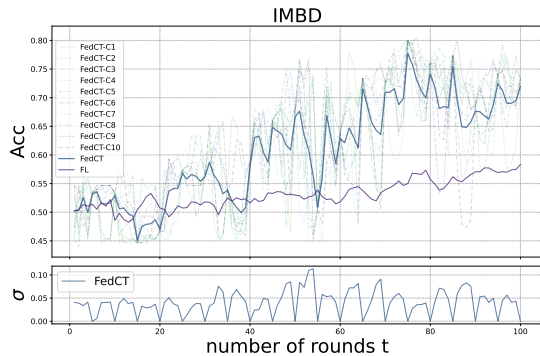


Figure 7: **Top:** Test accuracy (ACC) over time for GPT2 fine-tuning on IMBD with ACC of FL, and ACC of local models and their average for FEDCT. **Bottom:** Standard deviation of test accuracy of local models in FEDCT.

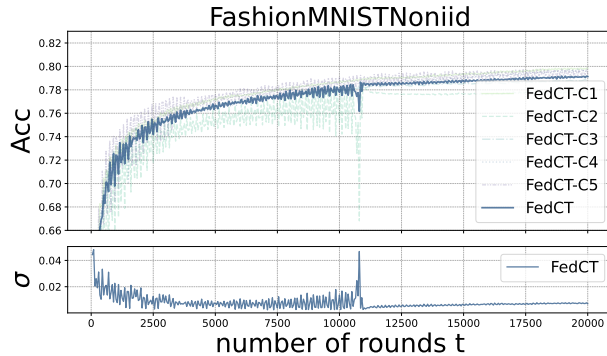


Figure 8: **Top:** Test accuracy (ACC) over time for $m = 5$ local models of FEDCT on heterogeneous distribution for the FashionMNIST dataset ($\alpha_1 = 100, \alpha_2 = 0.01$). **Bottom:** Standard deviation of test accuracy of local models in FEDCT.

of decision trees (DT), random forests (RF), rule ensembles (RuleFit), gradient-boosted decision trees (XGBoost), and neural networks (MLP). The results in Table 5 show that using a diverse ensemble of models can further improve accuracy. That is, using only XGBoost models on each client results in a test accuracy of 0.94 on the BreastCancer dataset, whereas using a heterogeneous ensemble yields a slightly higher test accuracy of 0.95. Note that for this experiment we tried a few random combinations of models for the heterogeneous ensemble. Optimizing the ensemble to further improve accuracy makes for excellent future work.

Dataset	C1	C2	C3	C4	C5	ACC
BreastCancer	DT	RF	RuleFit	XGBoost	RF	0.95 ± 0.001
BreastCancer	DT	MLP	RuleFit	XGBoost	RF	0.93 ± 0.002
BreastCancer	XGBoost	XGBoost	XGBoost	XGBoost	XGBoost	0.94 ± 0.001

Table 5: Mixed model experiment

D.2. Fine-Tuning Large Language Models (GPT2)

We now provide further details on our experiment on fine-tuning large language models via FEDCT. The rationale for this experiment was that fine-tuning should be a task particularly suitable to label sharing, since the quality of initial pseudo-labels will already be high, since model quality is good to begin with. In contrast, in standard learning scenarios the initial models will be of poor quality so that the first pseudo-labels will be fairly poor.

To test whether FEDCT performs well in a fine-tuning scenario, we fine-tune the GPT2 model transformer with a sequence classification head (linear layer) comprising of 124.44 million parameters on the IMDB sentiment classification dataset (Maas et al., 2011). We use $m = 10$ clients each with a local dataset of 145 examples and an unlabeled dataset of $|U| = 150$ examples. We use a test set of 150 examples for evaluation. We run fine-tuning for $T = 100$ rounds with a communication period of $b = 5$. Here, FEDCT achieves a test accuracy of 0.73, whereas FEDAVG in that case only achieves a test accuracy of 0.59.

We analyze the convergence in terms of test accuracy in Fig. 7. It shows that the initial accuracy is indeed already high, both for FEDCT and FEDAVG. Moreover, both methods exhibit a more linear convergence, in contrast to the saturating convergence behavior typical for standard learning tasks. The variance of individual clients in FEDCT is low right from the start, but drops substantially in each communication round and increases again afterwards. This suggests that local datasets are heterogeneous enough to have different local optima, which is likely, given the small training set sizes. This data heterogeneity could explain the suboptimal performance of FEDAVG, but leads to a conundrum: FEDCT performed worse than FEDAVG on strongly heterogeneous data. In the discussion (Sec. 6), we argued that an explanation why FEDCT performs poorly on strongly heterogeneous data is that label quality on average is poor, since some clients have not seen

Protecting Sensitive Data through Federated Co-Training

Dataset	FEDCT		DP-FEDCT		PATE		DP-PATE	
	ACC	VUL	ACC	VUL	ACC	VUL	ACC	VUL
CIFAR10	0.77 ± 0.003	0.52	0.76 ± 0.002	0.51	0.69 ± 0.002	0.60	0.67 ± 0.003	0.58
FashionMNIST	0.82 ± 0.004	0.51	0.80 ± 0.001	0.52	0.73 ± 0.001	0.59	0.73 ± 0.002	0.57
Pneumonia	0.76 ± 0.008	0.51	0.75 ± 0.004	0.51	0.75 ± 0.003	0.59	0.71 ± 0.001	0.58
MRI	0.63 ± 0.004	0.52	0.62 ± 0.002	0.51	0.61 ± 0.001	0.60	0.60 ± 0.001	0.57
SVHN	0.88 ± 0.002	0.53	0.86 ± 0.001	0.53	0.87 ± 0.002	0.58	0.86 ± 0.002	0.57

Table 6: Test Accuracy (ACC) and privacy Vulnerability (VUL) for $m = 5$ clients

a single example for some classes. If that explanation is correct, it would make sense that FEDCT performs well in a fine-tuning setting, even under strong data heterogeneity: the quality of labels will be high. As mentioned in the discussion, these results are promising and suggest that semi-supervised learning can be beneficial for fine-tuning in a federated setup. The experiments are preliminary, though, and therefore cannot be considered conclusive.

D.3. Comparison to PATE

PATE (Papernot et al., 2017) is a distributed (but not collaborative) distillation algorithm with the goal of producing a single student model from an ensemble of teachers, each teacher trained on a distributed dataset. The approach assumes a secure environment for distributed dataset and server to produce pseudo-labels for a public unlabeled dataset. An untrusted entity can then distill a student model using the pseudo-labeling. This differs from the setting we consider, where the server that aggregates predictions and produces the pseudo-label cannot necessarily be trusted, i.e., we assume the server to be honest-but-curious. Although the setting of PATE fundamentally differs from the setting we consider, comparing FEDCT and PATE is interesting: both approaches produce a pseudo-labeling via a majority vote and train models using these pseudo-labels on a public unlabeled dataset. A major difference is that PATE trains teachers until convergence first, then produces the pseudo-labels, and finally trains the student on the pseudo-labeled public dataset alone. In FEDCT, clients iteratively train their models on the private training set in conjunction with the pseudo-labeled public dataset and update pseudo-labels in each communication round. Therefore, we expect FEDCT to achieve higher model quality than PATE.

It is noteworthy that PATE also offers a differential privacy mechanism on the shared information—in contrast to FEDCT, this shared information is not the local predictions, but rather the consensus labels produced by the server. PATE achieves differential privacy by using a variant of the Gaussian mechanism (Dwork et al., 2006) on the prediction counts for each class, i.e., for each example the prediction counts are the numbers of votes for a particular class from the clients. These counts are integer values, but not binary, and therefore a correctly calibrated Gaussian noise achieves Rényi differential privacy (see Thm. 6 on the GNMax Aggregator in (Papernot et al., 2017)). We compare both FEDCT and DP-FEDCT to PATE and its differentially private variant DP-PATE. The results in Table 6 for $m = 5$ clients/teachers show that, indeed, collaborative training (FEDCT) achieves substantially higher test accuracy than distillation (PATE). Surprisingly, sharing hard labels of each client (FEDCT) results in a slightly lower vulnerability score (VUL) than sharing the pseudo-labels (PATE). One possible explanation is that in PATE, teachers are trained until full convergence which might lead teachers to overfit the local training data. Therefore, their shared information might reveal more about the training data, since membership attacks tend to be more effective when a model is overfitted (Shokri et al., 2017). We furthermore observe that both FEDCT and PATE are robust to their respective differential privacy mechanisms, since both DP-FEDCT and DP-PATE achieve a test accuracy similar to their non-differentially-private variants.

In Tab. 7 we investigate the scalability of FEDCT and PATE by testing both methods on $m = 100$ clients on the FashionMNIST and Pneumonia datasets. The results indicate that both methods achieve high accuracy also with a higher distribution of datasets and that the advantage of collaborative training (FEDCT) over simple distillation (PATE) remains.

Dataset	FEDCT	PATE
FashionMNIST	0.7154	0.6318
Pneumonia	0.7269	0.6903

Table 7: Test accuracy ACC of PATE Vs FEDCT for $m = 100$ clients

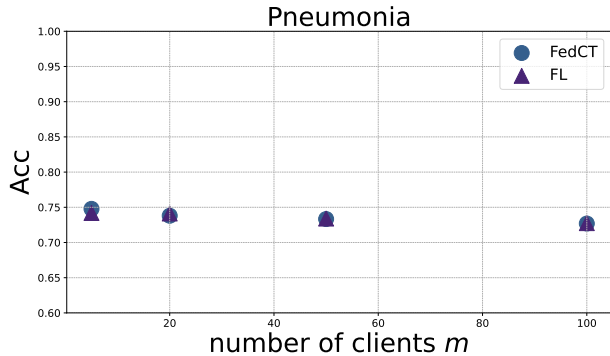


Figure 9: Test accuracy (ACC) of FEDCT and FEDAVG (FL) on Pneumonia with $|U| = 200$ for various numbers of clients m .

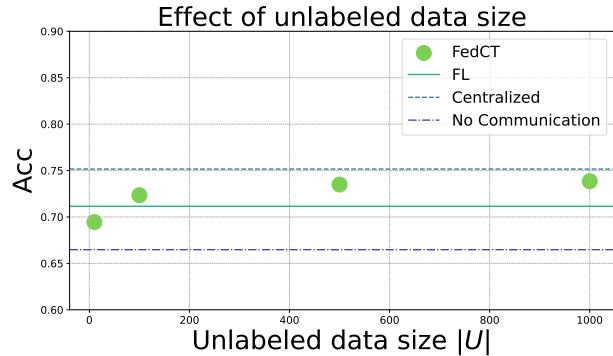


Figure 10: Test accuracy (ACC) of FEDCT under different unlabeled dataset size U .

D.4. Comparison to FedMD

We evaluate the performance of FEDCT on a scenario with heterogeneous data proposed by Li & Wang (2019). While this scenario is not compatible with our assumptions, since it assumes a public labeled dataset and it assumes that for both the private and public dataset each instance has two labels: a fine-grained class label, and a more coarse superclass label. An example of such a dataset is CIFAR100, where the 100 classes fall into 20 superclasses. Data heterogeneity is achieved by homogeneously distributing superclasses over clients, but in such a way that each client only observes a single class per superclass. This means, while all clients observe vehicles, some only observe cars, others only bicycles. The classification task is to predict the superclass. This should ensure that a meaningful consensus can be achieved. We compare FEDCT to the method Li & Wang (2019) proposed for this scenario (FedMD). Here, FEDCT achieves a test accuracy of 0.51, slightly outperforming FedMD which achieves a test accuracy of 0.50. We do not compare privacy, since FedMD is algorithmically equivalent to DD using a central server.

D.5. Additional Results on Scalability

To ensure the positive scalability results in our experiments section are not an outlier particular to the FashionMNIST dataset, we here report the test accuracy wrt. the number of clients on the Pneumonia dataset, as well. The results in Figure 9 show that also on this dataset FEDCT scales as well as FEDAVG with the number of clients. This indicates that FEDCT indeed scales well with the number of clients.

D.6. Ablation Study

We want to investigate the effect of co-training on the performance. For that, we first analyze the effect of sharing predictions on the unlabeled dataset by evaluating the performance of FEDCT on varying sizes of U . We then investigate the effect of collaboration by comparing the performance of FEDCT and FEDAVG to local training without communication.

Effect of the Size of the Unlabeled Dataset: Since FEDCT utilizes a public unlabeled dataset, a natural question is how large this unlabeled dataset needs to be. To answer this question, we evaluate the performance of FedCT for varying sizes $|U|$ of the unlabeled dataset. We evaluate FEDCT on the Pneumonia dataset where we fixed the local training data set size to 100 examples. Our results in Fig. 10 show that with $|U| = 100$ examples we reach high model quality, comparable to FEDAVG, and that further increasing $|U|$ only slightly improves model quality. Using too little unlabeled examples, however, does negatively impact FEDCT. This indicates, that FEDCT indeed utilizes the unlabeled dataset. To further investigate this, we compare FEDCT also to training local models without communication and pooling all data for centralized training. Indeed, FEDCT even with a small unlabeled dataset outperforms local training without communication. Moreover, with $|U| = 1000$ FEDCT nearly reaches the model quality of centralized training.

Effect of Collaboration: Our experiments so far show that the collaboration via co-training is as effective as the collaboration via model averaging. A natural question then is: is collaboration necessary at all? In particular, since DP-

FEDCT achieves a good performance even with a lot of noise on local predictions (corresponding to a small ϵ). To test this, we compare FEDCT and FEDAVG with local training without any communication. We use the same setup as in our main experiment from Tab. 1 and report the average test accuracy of local models over three runs in Tab. 8. We included the results of FEDCT and FEDAVG from Tab. 1 for comparison. These results show that collaboration substantially improves test accuracy over no-communication—on average by 0.11. Therefore, collaboration is indeed indeed beneficial, which supports our hypothesis that the good performance of DP-FEDCT even under strong DP noise is due to the robustness of majority voting to noise, as Papernot et al. (2017) suggested as well.

Dataset	no-communication	FEDCT	FEDAVG
CIFAR10	0.73 ± 0.003	0.77 ± 0.003	0.77 ± 0.020
FashionMNIST	0.79 ± 0.005	0.82 ± 0.004	0.83 ± 0.024
Pneumonia	0.68 ± 0.004	0.76 ± 0.008	0.74 ± 0.013
MRI	0.42 ± 0.001	0.63 ± 0.004	0.66 ± 0.015
SVHN	0.76 ± 0.002	0.88 ± 0.002	0.91 ± 0.026

Table 8: Test accuracy (ACC) for $m = 5$ clients on iid data.

E. Details on Experiments

E.1. Details on Privacy Vulnerability Experiments

We measure privacy vulnerability by performing membership inference attacks against FEDCT, FEDAVG, DD, and PATE. In all attacks, the attacker creates an attack model using a model it constructs from its training and test datasets. Similar to previous work (Shokri et al., 2017), we assume that the training data of the attacker has a similar distribution to the training data of the client. Once the attacker has its attack model, it uses this model for membership inference using ShadowMetric developed by (Shokri et al., 2017). In blackbox attacks (in which the attacker does not have access to intermediate model parameters), it only uses the classification scores it receives from the target model (i.e., client’s model) for membership inference. On the other hand, in whitebox attacks (in which the attacker can observe the intermediate model parameters), it can use additional information in its attack model. Since the proposed FEDCT, DD and PATE do not reveal intermediate model parameters to any party, it is only subject to blackbox attacks. Vanilla federated learning on the other hand is subject to whitebox attacks. Each inference attack produces a membership score of a queried data point, indicating the likelihood of the data point being a member of the training set. We measure the success of membership inference as ROC AUC of these scores. The **vulnerability (VUL)** of a method is the ROC AUC of membership attacks over K runs over the entire training set (also called attack epochs) according to the attack model and scenario. A vulnerability of 1.0 means that membership can be inferred with certainty, whereas 0.5 means that deciding on membership is a random guess.

We assume the following attack model: clients are honest and the server may be semi-honest (follow the protocol execution correctly, but it may try to infer sensitive information about the clients). The main goal of a semi-honest server is to infer sensitive information about the local training data of the clients. This is a stronger attacker assumption compared to a semi-honest client since the server receives the most amount of information from the clients during the protocol, and a potential semi-honest client can only obtain indirect information about the other clients. We also assume that parties do not collude.

The attack scenario for FEDCT, DD and PATE is that the attacker can send a (forged) unlabeled dataset to the clients and observe their predictions, equivalent to one attack epoch ($K = 1$); the one for FEDAVG and DP-FEDAVG is that the attacker receives model parameters and can run an arbitrary number of attacks—we use $K = 500$ attack epochs.

E.2. Datasets

We use 3 standard image classification datasets: CIFAR10 (Krizhevsky et al., 2010), FashionMNIST (Xiao et al., 2017), IMDB (Maas et al., 2011) and SVHN (Netzer et al., 2011). We describe the datasets and our preprocessing briefly.

CIFAR10 consists of 50 000 training and 10 000 test 32×32 color images in 10 classes with equal distribution (i.e., a total of 6 000 images per class). Images are normalized to zero mean and unit variance. *FashionMNIST* consists of 60 000 training and 10 000 test 28×28 grayscale images of clothing items in 10 classes with equal distribution. Images are not normalized. *SVHN* (Street View House Numbers) consists of 630 420 32×32 color images of digits from house numbers in Google

Street View, i.e., 10 classes. The dataset is partitioned into 73 257 for training, 26 032 for testing, and 531 131 additional training images. In our experiments, we use only the training and testing set. Images are not normalized.

IMBD sentimental dataset consists of a large collection of movie reviews along with corresponding sentiment labels indicating whether the sentiment expressed in each review is positive or negative. A total of 1750 examples have been used. 1450 examples as a training set, 150 examples as a testing set and 150 examples as unlabeled dataset.

We use five standard datasets from the UCI Machine Learning repository for our experiments on collaboratively training interpretable models: *WineQuality* (Cortez et al., 2009), *BreastCancer* (Sudlow et al., 2015), *AdultsIncome* (Becker & Kohavi, 1996), *Mushroom* (Bache & Lichman, 1987), and *Covertypes* (Blackard, 1998). A short description of the five datasets follows. *WineQuality* is a tabular dataset of 6 497 instances of wine with 11 features describing the wine (e.g., alcohol content, acidity, pH, and sulfur dioxide levels) and the label is a wine quality score from 0 to 10. We remove duplicate rows and transform the categorical type attribute to a numerical value. We then normalize all features to zero mean and unit variance. *BreastCancer* is a medical diagnostics tabular dataset with 569 instances of breast cell samples with 30 features describing cell nuclei with 2 classes (malignant and benign). We followed the same preprocessing steps as *WineQuality* dataset. *AdultIncome* is a tabular dataset with 48, 842 instances of adults from various backgrounds with 14 features describing attributes such as age, work class, education, marital status, occupation, relationship, race, gender, etc. The dataset is used to predict whether an individual earns more than 50, 000\$ a year, leading to two classes: income more than 50, 000\$, and income less than or equal to 50, 000\$. *Mushroom* is a biological tabular dataset with 8124 instances of mushroom samples with 22 features describing physical characteristics such as cap shape, cap surface, cap color, bruises, odor, gill attachment, etc. The dataset is used to classify mushrooms as edible or poisonous, leading to two classes: edible and poisonous. *Covertypes* is an environmental tabular dataset with 581, 012 instances of forested areas with 54 features describing geographical and cartographical variables, such as elevation, aspect, slope, horizontal distance to hydrology, vertical distance to hydrology, horizontal distance to roadways, hillshade indices, and wilderness areas and soil type binary indicators. The dataset is used to predict forest cover type, leading to 7 distinct classes: Spruce/Fir, Lodgepole Pine, Ponderosa Pine, Cottonwood/Willow, Aspen, Douglas-fir, and Krummholz.

Furthermore, we use 2 medical image classification datasets, *Pneumonia* (Kermany et al., 2018), and *MRI*⁶. *Pneumonia* consists of 5 286 training and 624 test chest x-rays with labels *normal*, *viral pneumonia*, and *bacterial pneumonia*. We simplify the labels to *healthy* and *pneumonia* with a class imbalance of roughly 3 pneumonia to 1 healthy. The original images in the *Pneumonia* dataset do not have a fixed resolution as they are sourced from various clinical settings and different acquisition devices. We resize all images to a resolution of 224×224 pixels without normalization. *MRI* consists of 253 MRI brain scans with a class imbalance of approximately 1.5 brain tumor scans to 1 healthy scan. Out of the total 253 images, we use 53 images as testing set. Similar to the pneumonia dataset, the original images have no fixed resolution and are thus resized to 150×150 without normalization.

E.3. Experimental Setup

We now describe the details of the experimental setup used in our empirical evaluation.

In our privacy-utility trade-off experiments, we use $m = 5$ clients for all datasets. We report the split into training, test, and unlabeled dataset per dataset, as well as the used communication period b and number of rounds T in Table 9. For the scalability experiments, we use the same setup, varying $m \in \{5, 10, 20, 40, 80\}$ clients. For the experiments on heterogeneous data distributions, we use the same setup as for the privacy-utility trade-off, but we sample the local dataset

⁶<https://www.kaggle.com/datasets/navoneel/brain-mri-images-for-brain-tumor-detection>

Dataset	training size	testing size	unlabeled size $ U $	communication period b	number of rounds T
CIFAR10	$40 \cdot 10^3$	$10 \cdot 10^3$	$10 \cdot 10^3$	10	$3 \cdot 10^3$
FashionMNIST	$10 \cdot 10^3$	$10 \cdot 10^3$	$50 \cdot 10^3$	50	$20 \cdot 10^3$
Pneumonia	4386	624	900	20	$20 \cdot 10^3$
MRI	30	53	170	6	$2 \cdot 10^3$
SVHN	38 257	26 032	$35 \cdot 10^3$	10	$20 \cdot 10^3$
IMDB	1450	150	150	5	100

Table 9: Dataset descriptions for image classification experiments.

Layer	Output Shape	Activation	Parameters
Conv2D	(32, 32, 32)	ReLU	896
BatchNormalization	(32, 32, 32)	-	128
Conv2D	(32, 32, 32)	ReLU	9248
BatchNormalization	(32, 32, 32)	-	128
MaxPooling2D	(16, 16, 32)	-	-
Dropout	(16, 16, 32)	-	-
Conv2D	(16, 16, 64)	ReLU	18496
BatchNormalization	(16, 16, 64)	-	256
Conv2D	(16, 16, 64)	ReLU	36928
BatchNormalization	(16, 16, 64)	-	256
MaxPooling2D	(8, 8, 64)	-	-
Dropout	(8, 8, 64)	-	-
Conv2D	(8, 8, 128)	ReLU	73856
BatchNormalization	(8, 8, 128)	-	512
Conv2D	(8, 8, 128)	ReLU	147584
BatchNormalization	(8, 8, 128)	-	512
MaxPooling2D	(4, 4, 128)	-	-
Dropout	(4, 4, 128)	-	-
Flatten	(2048,)	-	-
Dense	(128,)	ReLU	262272
BatchNormalization	(128,)	-	512
Dropout	(128,)	-	-
Dense	(10,)	Linear	1290

Table 10: CIFAR10 architecture

Layer	Output Shape	Activation	Parameters
Flatten	(784,)	-	-
Linear	(784, 512)	-	401,920
ReLU	(512,)	ReLU	-
Linear	(512, 512)	-	262,656
ReLU	(512,)	ReLU	-
Linear	(512, 10)	-	5,130

Table 11: FashionMNIST architecture

from a Dirichlet distribution as described in the main text.

For all experiments, we use Adam as an optimization algorithm with a learning rate 0.01 for CIFAR10, and 0.001 for the remaining datasets. A description of the DNN architecture for each dataset follows.

The neural network architectures used for each dataset are given in the following. For CIFAR10 we use a CNN with multiple convolutional layers with batch normalization and max pooling. The details of the architecture are described in Table 10. For FashionMNIST, we use a simple feed forward architecture on the flattened input. The details of the architecture are described in Table 11. For Pneumonia, we use a simple CNN, again with batch normalization and max pooling, with details given in Table 12. For MRI we use an architecture similar to pneumonia with details described in Table 13. For SVHN, we use again a standard CNN with batch normalization and max pooling, detailed in Table 14.

For our experiments on interpretable models, we use $m = 5$ clients. For decision trees (DT), we split by the Gini index with at least 2 samples for splitting. For RuleFit, we use a tree size of 4 and a maximum number of rules of 200. For the WineQuality dataset, we use an unlabeled dataset size of $|U| = 4100$, a training set size of 136, and a test set size of 1059. For BreastCancer, we use an unlabeled dataset of size $|U| = 370$, a training set of size 85, and a test set of size 114. For the AdultsIncome dataset, we use an unlabeled dataset of size $|U| = 10^4$, a training set of size 31,073, and a test set of size 7769. For the Mushroom dataset, we use an unlabeled dataset of size $|U| = 4000$, a training set of size 2499, and a test set

Layer	Output Shape	Activation	Parameters
Conv2d	(3, 32, 32)	-	896
BatchNorm2d	(32, 32, 32)	-	64
Conv2d	(32, 32, 32)	-	18,464
BatchNorm2d	(64, 32, 32)	-	128
MaxPool2d	(64, 16, 16)	-	-
Conv2d	(64, 16, 16)	-	36,928
BatchNorm2d	(64, 16, 16)	-	128
MaxPool2d	(64, 8, 8)	-	-
Flatten	(4096,)	-	-
Linear	(2,)	-	4,194,306

Table 12: Pneumonia architecture

Layer	Output Shape	Activation	Parameters
Conv2d	(3, 32, 32)	-	896
BatchNorm2d	(32, 32, 32)	-	64
Conv2d	(32, 32, 32)	-	18,464
BatchNorm2d	(64, 32, 32)	-	128
MaxPool2d	(64, 16, 16)	-	-
Conv2d	(64, 16, 16)	-	36,928
BatchNorm2d	(64, 16, 16)	-	128
MaxPool2d	(64, 8, 8)	-	-
Flatten	(32768,)	-	-
Linear	(2,)	-	2,636,034

Table 13: MRI architecture

of size 1625. For the covertime dataset, we use an unlabeled dataset of size $|U| = 5 \cdot 10^4$, a training set of size 414,810, and a test set of size 116,202.

Layer	Output Shape	Parameters
Conv2d	(3, 32, 32)	896
BatchNorm2d	(32, 32, 32)	64
Conv2d	(32, 32, 32)	9,248
MaxPool2d	(32, 16, 16)	-
Dropout2d	(32, 16, 16)	-
Conv2d	(32, 16, 16)	18,464
BatchNorm2d	(64, 16, 16)	128
Conv2d	(64, 16, 16)	36,928
MaxPool2d	(64, 8, 8)	-
Dropout2d	(64, 8, 8)	-
Conv2d	(64, 8, 8)	73,856
BatchNorm2d	(128, 8, 8)	256
Conv2d	(128, 8, 8)	147,584
MaxPool2d	(128, 4, 4)	-
Dropout2d	(128, 4, 4)	-
Flatten	(2048,)	-
Linear	(128,)	262,272
Dropout	(128,)	-
Linear	(10,)	1,290

Table 14: SVHN architecture

Layer	Parameters
Embedding: 2-1	38,597,376
Embedding: 2-2	786,432
Dropout: 2-3	-
ModuleList: 2-4	-
GPT2Block: 3-1 to 3-12	7,087,872 (each)
LayerNorm: 2-5	1,536
Linear: 1-2	1,536
Total params	124,441,344

Table 15: GPT2ForSequenceClassification Model Architecture